GOSPODARKA SUROWCAMI MINERALNYMI – MINERAL RESOURCES MANAGEMENT

2026 Volume 42 Issue 3 Pages 5–46

DOI: 10.24425/gsm.2026.6002

ZHENYU WANG[1], ZHENGYAO LI[2], ANHUA ZOU[3], XIN GAO[4], ZUCHAO PAN[5]

A new process for high-efficiency rare earth enrichment in Baiyun Ebo metal ores: a synergistic optimization study of open-circuit flotation, closed-circuit flotation of the middle ore and magnetic separation

Introduction

Rare Earth Elements (REEs), denoted as RE (Hu et al. 2025), encompass a group of seventeen metallic elements consisting of the lanthanides plus scandium and yttrium from

✉ Corresponding Author: Zhengyao Li; e-mail: zyli0213@ustb.edu.cn

[1] Key Laboratory of Ministry of Education for Efficient Mining and Safety of Metal Mines, University of Science and Technology Beijing, Beijing, China; School of Resources and Safety Engineering, University of Science and Technology Beijing, Beijing, China; ORCID iD: 0000-0002-2242-3325

[2] Key Laboratory of Ministry of Education for Efficient Mining and Safety of Metal Mines, University of Science and Technology Beijing, Beijing, China; School of Resources and Safety Engineering, University of Science and Technology Beijing, Beijing, China; e-mail: zyli0213@ustb.edu.cn

[3] Key Laboratory of Ministry of Education for Efficient Mining and Safety of Metal Mines, University of Science and Technology Beijing, Beijing, China; School of Resources and Safety Engineering, University of Science and Technology Beijing, Beijing, China; e-mail: zouanhua.bj@163.com

[4] Zhongye Changtian International Engineering Co., Ltd., China

[5] Key Laboratory of Ministry of Education for Efficient Mining and Safety of Metal Mines, University of Science and Technology Beijing, Beijing, China; School of Resources and Safety Engineering, University of Science and Technology Beijing, Beijing, China

Group IIIB of the periodic table. Globally recognized as strategic resources (Kanazawa and Kamitani 2006; Duta et al. 2016; Wang et al. 2023), they are extensively applied in high-technology fields (Xingyi et al. 2008; Goldschmidt and Fischer 2015; Mengmeng 2024) and are often referred to as "industrial vitamins" and "versatile soil" (Hongrui et al. 2020; Chunhua and Xiaowei 2024). Statistics indicate that the world's total rare earth reserves are approximately 120 million tons. Countries with relatively abundant reserves, in descending order, are China, Vietnam, Brazil, Russia, and India, collectively accounting for 90% of the total. China possesses the largest reserves, amounting to 44 million tons, representing over one-third of the global total. Figure 1 shows the global distribution of rare earth resources based on the United States Geological Survey 2024 report.

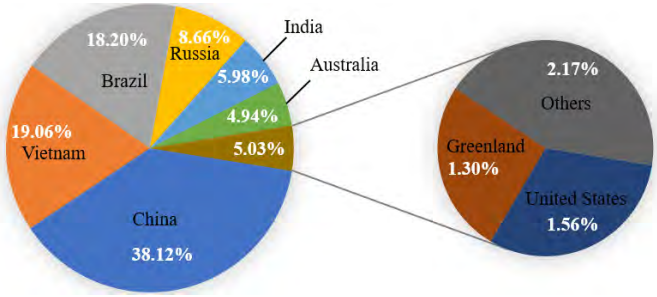

Fig. 1. Global rare earth resources distribution, U.S. Geological Survey, 2024

Rys. 1. Globalny rozkład zasobów pierwiastków ziem rzadkich

The distribution of China's rare earth deposits exhibits a distinct "light REEs in the north, heavy REEs in the south" geographical pattern (Wei et al. 2023). Light rare earth deposits are primarily located in Inner Mongolia and Shandong, while heavy rare earth resources are concentrated in southern regions such as Jiangxi (Sujiang et al. 2020). To achieve comprehensive utilization of rare earth resources, beneficiation processes that fail to meet production requirements are being progressively phased out. The Bayan Obo mining district, recognized as the world's largest Fe-Nb-REE polymetallic deposit, contains mixed rare earth reserves of 35 million tons. The predominant rare earth minerals (bastnaesite and monazite) are embedded in fine particle size, presenting significant processing challenges. The current concentrator operation employs an open-circuit "one roughing-two cleaning" flotation circuit for Rare Earth Oxide (REO) recovery, yielding a concentrate averaging 55% grade with 45% recovery. The overall resource utilization rate remains below 17.9%, underscoring the urgent need for technological innovation to improve beneficiation performance.

Beneficiation methods for rare earth ores primarily consist of gravity separation (a physical separation method that utilizes gravity or centrifugal force to achieve the separation of heavy and light minerals), magnetic separation (a physical separation method that utilizes differences in magnetic properties between minerals to separate magnetic minerals from non-magnetic

ones in an inhomogeneous magnetic field), and flotation (a mineral processing method that utilizes differences in the physicochemical properties of mineral surfaces to achieve separation). Owing to the diverse geological genesis of rare earth deposits, single-process beneficiation techniques often yield unsatisfactory results and fail to achieve target product quality specifications. Therefore, integrated process flowsheets combining two or more beneficiation methods are generally employed to produce high-grade rare earth concentrates. The principal combined processes currently utilized in rare earth separation include:

1) magnetic-gravity separation (Liu et al. 2016),
2) gravity-flotation (Qiu et al. 2015),
3) magnetic-flotation (Zhang et al. 2017; Xiong et al. 2015, 2018),
4) magnetic-gravity-flotation (Chen et al. 2013; Wang et al. 2017),

as summarized in Table 1. The magnetic-flotation combined process demonstrates the most extensive industrial application owing to its superior separation performance. Significant advances have been achieved through novel reagent schemes: Researchers, including Wenliang Xiong et al. (2018) and Xiaojuan He et al. (2002), developed specialized collectors; Fangji Li et al. (2002), Yanbo Xu et al. (2020), and Chunhui Zhao et al. (2000) reported improved performance using mixed collector systems; and effective depression was achieved with combined modifiers such as citric acid-sodium silicate (Wang et al. 2013) and sodium silicate-ferrous sulfate (Xiomg and Ma 2003), as detailed in Table 2. Despite these advancements, substantial potential remains for enhancing overall rare earth resource utilization rates.

Based on the process mineralogy characteristics of the Bayan Obo rare earth ore, systematic open-circuit flotation tests were conducted on the raw ore. According to the liberation properties of the rare earth middlings, systematic flotation tests were performed

Table 1. Separation efficiency of REO under different combined processes

Tabela 1. Skuteczność oddzielania REO w różnych procesach łączonych

Number	Primary grade of the REO/%	Combined process	REO concentrate	
			grade/%	recovery/%
1	0.28	Magnetic-gravity separation (Liu et al 2016)	1.51	83.21
2	6.62	Gravity separation – flotation (Qiu et al 2015)	60.37	86.68
3	6.02	Magnetic separation – flotation (Yue et al 2017)	74.14	66.56
4	2.40	Flotation – magnetic separation (Xiong et al. 2018)	65.00	55.00
5	6.53	Flotation – magnetic separation (Xu et al 2015)	46.12	52.20
6	1.57	Magnetic separation – gravity separation – flotation (Yong et al 2013)	47.85	61.50
7	2.16	Magnetic separation – gravity separation – flotation (Wang et al 2017)	65.39	83.26

Table 2. Separation efficiency of REO under different flotation reagent

Tabela 2. Skuteczność separacji REO przy zastosowaniu różnych odczynników flotacyjnych

Number	Primary grade of the REO/%	Combined process	REO concentrate	
			grade/%	recovery/%
1	1.46	Collector (RFS) (Xiong et al. 2018)	23.25	78.03
2	17.01	Collector (modified alkyl hydroxamic acid) (He et al. 2016)	25.03	77.68
3	9.01	Mixed collector (L102) (Li et al. 2002)	63.31	88.36
4	96.17	Mixed collector (OHA + NaOL) (Xu et al. 2020)	/	94.02
5	9.62	Collector (LF-8), Frother (LF-6) (Zhao et al. 2000)	60.63	63.89
6	8.45	Mixed depressant (sodium silicate + citric acid) (Wang et al. 2013)	51.32	70.94
7	3.13	Mixed depressant (sodium silicate + ferrous sulfate) (Xiong and Ma 2003)	62.57	79.06

after fine grinding. Furthermore, based on the magnetic differences among various minerals in the closed-circuit flotation concentrate, magnetic separation was employed to separate weakly magnetic rare earth oxides from other minerals. This combined process ultimately produces high-quality rare earth products and provides a scientific basis for improving the onsite beneficiation process.

1. Materials and methods

1.1. Materials and reagents

1.1.1. Rare earth ore

The rare earth ore used in the experimental study of this research was collected from the Bayan Obo mining area in Inner Mongolia, China, with 90.05% of the material passing 74 μm. The chemical multi-element analysis of the rare earth ore is shown in Table 3. The rare earth ore contains a variety of elements, with silicon dioxide having the highest relative content of 25.77%, REO accounting for 11.35%, and iron content of 15.12%. Based on the XRD analysis results of the rare earth ore shown in Figure 2, the main rare earth minerals are bastnaesite and monazite. The iron minerals include magnetite, hematite, and pyrite, while the gangue minerals are primarily aegirine, fluorite, apatite, quartz, and mica.

Table 3. Chemical composition analysis of the rare earth ore

Tabela 3. Analiza składu chemicznego rudy metali ziem rzadkich

Components	REO	Na_2O	MgO	CaO	BaO	SiO_2	ThO_2	Al_2O_3
Content (%)	11.35	4.88	1.12	14.55	2.97	25.77	0.043	0.81
Components	K_2O	Nb_2O_5	F	P	S	TFe	C	LOI
Content (%)	0.45	0.031	8.57	1.29	1.04	15.12	1.33	10.68

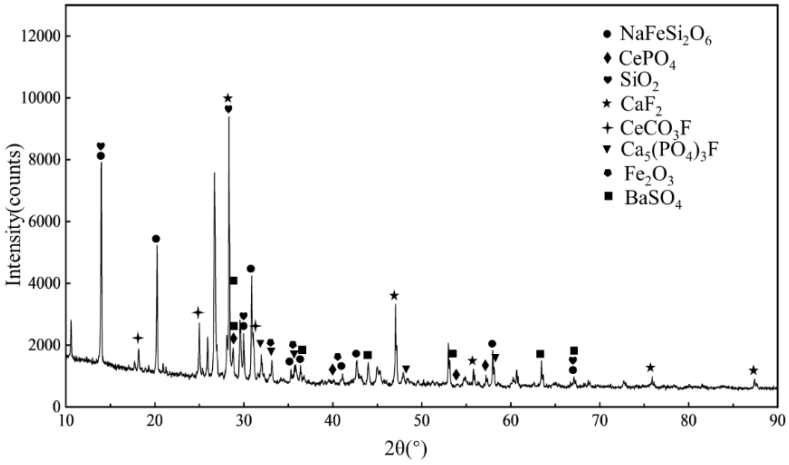

Fig. 2. XRD pattern of rare earth ore

Rys. 2. Wzór dyfrakcyjny rudy metali ziem rzadkich

1.1.2. Pure mineral

High-grade samples of bastnaesite, fluorite, and barite were obtained from the Bayan Obo mining district. The samples were characterized by X-ray diffraction (XRD) and inductively coupled plasma optical emission spectrometry/mass spectrometry (ICP-OES/MS). The XRD patterns are presented in Figure 3, and the chemical analysis results from ICP-OES/MS are summarized in Tables 4–6.

Table 4. Analysis results of chemical components of fluorite

Tabela 4. Wyniki analizy składu chemicznego fluorytu

Components	CaO	F	SiO_2	Fe_2O_3	SrO
Content (%)	81.00	18.88	0.05	0.03	0.02

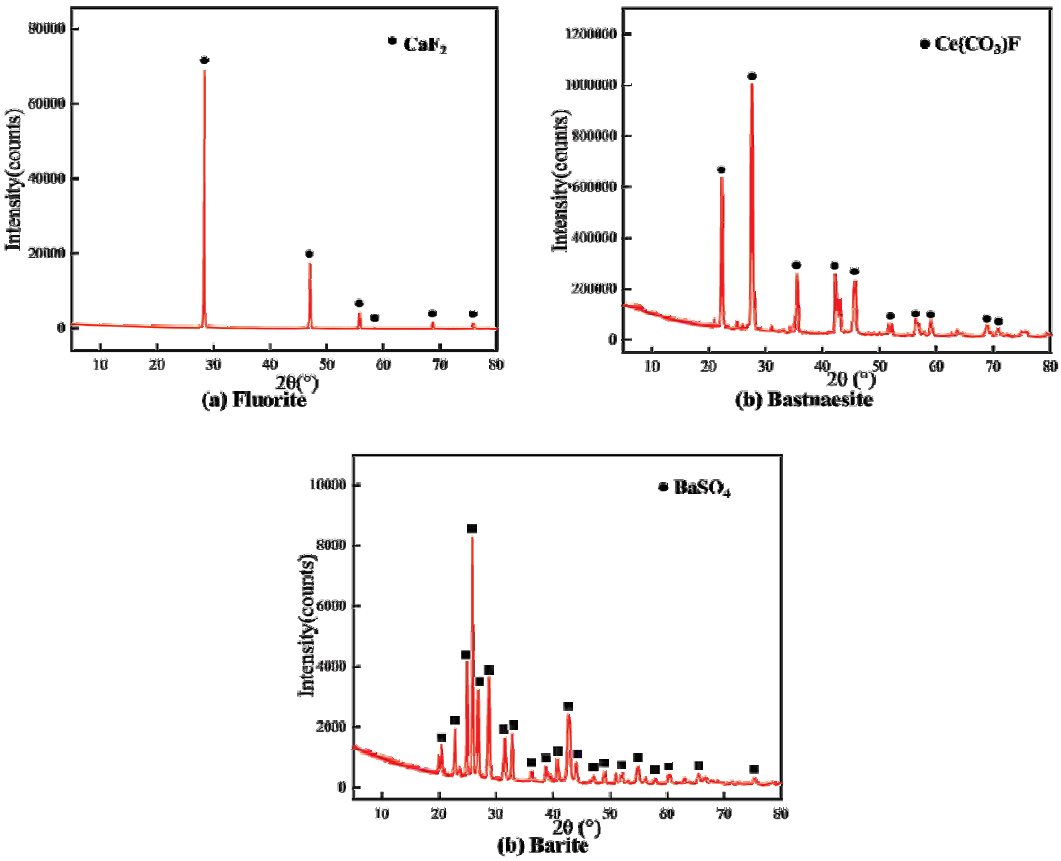

Fig. 3. XRD pattern of pure mineral
a – fluorite , b – bastnaesite , c – barite

Rys. 3. Wzór dyfrakcyjny czystych minerałów
a – fluoryt, b – bastnazyt, c – baryt

Table 5. Analysis results of chemical components of bastnaesite

Tabela 5. Wyniki analizy składu chemicznego bastnazytu

Components	CeO_2	La_2O_3	F	Nd_2O_3	Gd_2O_3	Pr_2O_3	BaO	SO_3
Content (%)	45.56	26.82	7.81	4.40	3.53	2.97	2.34	1.48
Components	CaO	SiO_2	SrO	Fe_2O_3	Al_2O_3	P_2O_5	MgO	
Content (%)	1.37	1.22	0.91	0.77	0.49	0.17	0.16	

Table 6. Analysis results of chemical components of barite

Tabela 6. Wyniki analizy składu chemicznego barytu

Components	BaO	SO_3	SiO_2	Na_2O	Al_2O_3	SrO	P_2O_5	Fe_2O_3
Content (%)	64.72	32.30	1.80	0.38	0.35	0.31	0.07	0.07

Figure 3 indicates that the purity of bastnaesite exceeds 90%, while the purities of both fluorite and barite are greater than 98%. As shown in Tables 4, 5, and 6, quartz is identified as the primary gangue mineral in all three purified mineral samples. The quality of these samples meets the requirements for pure mineral flotation tests and chemical analysis.

1.1.3. Reagents

In the flotation tests, sodium carbonate served as the pulp pH modifier. The depressants included sodium silicate (water glass), BY5 (a composite depressant primarily composed of sodium silicate with citric acid as a secondary component), sodium carboxymethyl cellulose, and sodium fluorosilicate. All the aforementioned reagents were of chemical pure grade and sourced from Shanghai Aladdin Biochemical Technology Co., Ltd. The collectors used were BQ2, H203, and H205, while the frothers included methyl isobutyl carbinol (MIBC), No. 11 oil foaming agent ($11^{\#}$ oil), and terpenic oil ($2^{\#}$ oil). These flotation reagents were supplied by Tieling Flotation Reagent Co., Ltd. Aqueous solutions of reagents at varying concentrations were prepared, and deionized water with a resistivity of 18 MΩ·cm was used throughout the pure mineral flotation testing process.

1.2. Experimental methods

1.2.1. Process mineralogy analyzing system

The rare earth ore was dried using a WGL-625B infrared dryer, thoroughly mixed, and split to obtain a representative sample for testing. The mineral composition and content of the sample, as well as the dissemination characteristics of the rare earth minerals, were measured using a Process Mineralogy Automatic Analyzer (BPMA, BGRIMM Technology Group).

1.2.2. Inductively coupled plasma optical emission spectrometry/mass spectrometry analysis

Inductively Coupled Plasma Optical Emission Spectrometry/Mass Spectrometry (ICP-OES/MS) was employed to analyze the elemental content of the rare earth ore and key

elements in separation products during the tests. The process mainly included grinding, drying and weighing, digestion and dissolution, instrumental detection, and data processing of the test samples.

1.2.3. Rare earth ore flotation tests

An appropriate amount of rare earth ore was weighed and transferred to the flotation cell of an XFD_{IV}-0.75L heated flotation machine, followed by the addition of a suitable volume of water. The flotation machine speed was set to 1,992 r/min. The heating function was activated, and stirring began. When the pulp temperature reached the predetermined level, the pH modifier was added and stirred for 5 minutes, followed by the depressant for 5 minutes, then the collector for 5 minutes, and finally the frother for 2 minutes before aeration and froth scraping commenced. The aeration rate was set to 0.08 m^3/h. The froth scraping time was 5 minutes in the roughing stage, 4 minutes in the first two cleaning stages, 3 minutes in the last two cleaning stages, and 4 minutes in the scavenging stage.

The tailings from the cleaning stages and the concentrate from the scavenging stage were combined as rare earth middlings. A 300 g portion of the dried middlings was transferred to an ALC–1.5L vertical stirred mill with a grinding concentration of 50% and a feed-to-ball ratio of 0.6. The ceramic grinding media were proportioned as 1.2 mm : 1.8 mm : 2.4 mm : 3.0 mm = 1 : 2 : 6 : 1, and the mill speed was 2,400 rpm. Grinding was conducted for the predetermined duration. The ground product was transferred to the flotation cell of an XFD_{IV}-0.5L heated flotation machine, and an appropriate amount of water was added. The flotation parameters, including machine speed, reagent types, addition sequence, and stirring times, were consistent with those used in the rare earth ore flotation tests. The froth scraping time was 5 minutes in the roughing stage, 4 minutes in the first two cleaning stages, and 3 minutes in the last two cleaning stages during the middlings flotation.

1.2.4. Magnetic separation tests

Using the closed-circuit flotation concentrate as feed, a CP3-500 magnetic separator was first used to preliminarily remove strongly magnetic minerals at a field intensity of 0.6 T. An LHGC–100F periodic vertical ring high-gradient magnetic separator was then employed for open-circuit "one roughing-one scavenging" magnetic separation. The field intensity was set to 1.5 T during roughing and 1.7 T during scavenging, with a 2 mm matrix and a pulsation frequency of 50 Hz.

1.2.5. Pure mineral flotation tests

A 2 g sample of pure mineral was ultrasonically cleaned for 5 minutes. After filtration, the purified mineral was transferred to the flotation cell of an XFG_{II}-35 mL suspended tank flotation machine, and 30 mL of deionized water was added. The pH regulator was added

first and stirred for 2 minutes, followed by the depressant for 2 minutes, the collector for 2 minutes, and finally the frother for 1 minute. Froth was then scraped for 3 minutes to collect the froth product and the tailings.

1.2.6. FTIR spectroscopy measurements

Fourier Transform Infrared Spectroscopy (FTIR) was acquired using a 740FT-IR spectrometer. A 2.0 g sample of pure mineral (particle size < 2 μm) was placed in a 40 mL cell, and reagents were added according to the predetermined experimental scheme. After 40 minutes of interaction, the sample was filtered, washed three times with deionized water, and dried. Then, 0.003 g of the sample was mixed with 0.3 g of dried potassium bromide (KBr), ground, and pressed into a pellet for measurement.

1.2.7. Adsorption experiments

Adsorption capacity of reagents on mineral surfaces was determined by the residual concentration method using a GENESYS 180 ultraviolet spectrophotometer. Specifically, 2.0 g of pure mineral sample (particle size: 0.0374–0.075 mm) was weighed and placed in a 100 mL beaker. An appropriate amount of deionized water was added, and the mixture was subjected to ultrasonic cleaning for 5 minutes. After standing for 30 minutes, the supernatant was decanted. Then, 50 mL of deionized water was added to the beaker, followed by the addition of depressant BY5 and collector BQ2 according to the predetermined experimental scheme. The mixture was magnetically stirred for 10 minutes and allowed to stand for another 30 minutes. Finally, the supernatant was extracted using a syringe, filtered, and analyzed by spectral scanning with the ultraviolet spectrophotometer. The absorbance at the maximum absorption wavelength was recorded, and the residual reagent concentration in the filtrate was calculated based on the standard calibration curve of the reagent.

2. Process mineralogy analysis of the rare earth ore

2.1. Mineral composition and content analysis

To identify the host minerals of rare earth elements, BPMA was employed to quantitatively determine the mineral species and their contents in the rare earth ore. This analysis provides key scientific insights for subsequent process optimization and comprehensive resource utilization. The mineralogical analysis results of the rare earth ore are presented in Table 7.

Based on the XRD analysis results of the rare earth ore presented in Section 1.1.1 and the analytical data in Table 7, the mineral composition of the ore is determined to be complex,

Table 7. Mineral species and content of the rare earth ore

Tabela 7. Gatunki minerałów i zawartość rudy metali ziem rzadkich

Mineral	Bastnaesite	Monazite	Parasite	Huanghoite	Allanite	Fergusonite	Aeschynite
Relative content/%	7.39	3.16	0.84	0.96	0.48	0.01	0.10
Mineral	Baotite	Columbite	Pyrochlore	Apatite	Fluorite	Dolomite	Calcite
Relative content/%	0.33	0.02	0.12	5.30	13.55	0.16	4.07
Mineral	Magnetite/Hematite	Pyrite	Siderite	Ilmenite	Feldspar	Pyrope	Quartz
Relative content/%	2.64	0.71	0.55	0.59	0.80	0.95	5.14
Mineral	Aergine	Pyroxene	Mica	Barite	Others		
Relative content/%	35.92	3.91	6.53	3.12	2.65		

containing over 20 distinct mineral species. Rare earth minerals are predominantly bastnaesite and monazite, with a combined content of 10.55%, representing over 85% of the total rare earth mineral content. Iron-bearing minerals, including magnetite, hematite, and pyrite, constitute 4.51% of the ore. The gangue minerals are primarily carbonate and silicate minerals, specifically comprising aegirine, fluorite, apatite, mica, quartz, calcite, pyroxene, barite, among others, with a collective content of 77.54%.

2.3. REO distribution across particle size fractions

If the REOs are concentrated in a specific intermediate particle size fraction, it indicates preliminary liberation of the rare earth minerals, providing a basis for determining the optimal grinding fineness. If REO is enriched in the ultra-fine fraction, it suggests the need to optimize the comminution process or implement early desliming as a pretreatment for the rare earth ore. Conversely, if the REO content remains high in the coarse fraction, it signifies insufficient mineral liberation, necessitating intensified grinding. Therefore, to reveal the distribution pattern of REO across different particle size fractions, standard sieve analysis coupled with ICP-OES/MS was employed to quantitatively analyze the REO content in each fraction of the ore. This analysis provides a scientific basis for formulating an efficient beneficiation process, avoiding excessive loss of rare earth resources, and improving overall REO recovery. The results are presented in Table 8.

Table 8. Relationship between REO distribution and particle size in the rare earth ore

Tabela 8. Zależność między rozkładem REO a wielkością cząstek w rudzie metali ziem rzadkich

Particle size (mm)	Yield (%)	REO grade (%)	REO distribution (%)	Cumulative yield (%)
≥0.074	5.22	1.14	0.50	100.00
0.053~0.074	12.92	3.29	3.58	94.78
0.045~0.053	10.24	5.21	4.50	81.86
0.038~0.045	6.55	6.55	3.62	71.62
0.020~0.038	32.51	12.11	33.21	65.07
≤0.020	32.56	19.88	54.59	32.56

Data in Table 8 indicate that the REO grade in the rare earth ore increases from 1.14% to 19.88% as the particle size decreases. The cumulative yield of the –38 μm fraction reaches 65.07%, with a cumulative REO distribution rate of 87.80%. These results demonstrate that rare earth elements are predominantly concentrated in the fine size fractions, indicating an

extremely fine dissemination size of the rare earth minerals. During flotation, a portion of the REO may report to the middlings and tailings due to incomplete liberation. Therefore, increasing the number of scavenging stages and implementing regrinding-recleaning of the rare earth middlings could be effective strategies to improve the grade of the rare earth concentrate.

2.4. Dissemination characteristics of the principal rare earth minerals

Based on the data in Table 8, bastnaesite and monazite collectively account for over 85% of the total rare earth minerals, confirming their role as the primary hosts of rare earth elements. Consequently, their dissemination characteristics fundamentally govern the overall beneficiation strategy and define the theoretical maximum for REO recovery. Focusing the research on these two minerals is therefore both rational and necessary. Although the study of minor rare earth minerals holds academic value, its impact on overall process efficiency is negligible. The dissemination characteristics of these two key minerals were analyzed using BPMA, with the dissemination size distribution presented in Table 9 and the liberation degree and intergrowth characteristics detailed in Table 10.

Table 9. Dissemination size of bastnaesite and monazite

Tabela 9. Wielkość cząstek bastnazytu i monacytu

Particle size (mm)	Bastnaesite		Monazite	
	distribution rate/%	cumulative passing distribution /%	distribution rate/%	cumulative passing distribution /%
≥0.038	13.25	100.00	2.21	100.00
0.020~0.038	36.80	86.75	26.35	97.79
0.015~0.020	15.71	49.95	20.57	71.44
0.010~0.015	17.77	34.24	25.01	50.87
0.005~0.010	13.43	16.48	21.07	25.87
≤0.005	3.05	3.05	4.80	4.80

Based on the data presented in Table 10, the cumulative passing distribution of bastnaesite particles with a size less than 38 μm is 86.75%, with 16.48% of particles finer than 10 μm. For monazite, the cumulative passing distribution below 38 μm reaches 97.79%, and 25.87% of particles are below 10 μm. These results further confirm the fine dissemination size of both bastnaesite and monazite, consequently indicating that direct flotation without prior grinding would be ineffective for achieving complete recovery of these minerals.

Table 10. Dissociation degree and continuous characteristics of bastnaesite and monazite

Tabela 10. Stopień dysocjacji i właściwości ciągłe bastnazytu i monacytu

Mineral	Liberated (%)	Mineral intergrowth					
		fluorite (%)	apatite (%)	iron minerals (%)	carbonate minerals (%)	silicate minerals (%)	others (%)
Bastnaesite	60.46	5.59	6.96	4.05	4.88	9.83	8.23
Monazite	54.20	3.21	3.47	7.63	4.16	12.77	12.46

According to the data in Table 10, over half of the bastnaesite exists in liberated form, with a liberation degree of 60.46%, while the total proportion of its intergrowths is 31.31%. Similarly, more than half of the monazite is liberated (54.20%), with intergrowths accounting for 33.34% of its total occurrence.

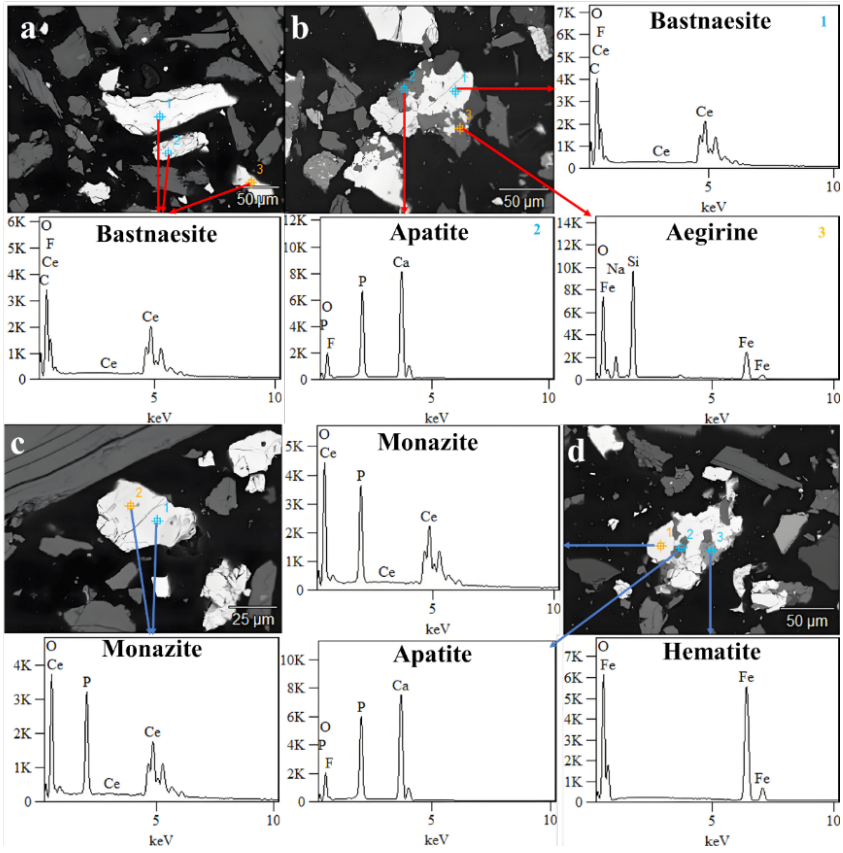

Fig. 4. Characterization of cerium fluorocarbon and monazite occurrence

Rys. 4. Charakterystyka występowania fluorowęglowodoru ceru i monacytu

Bastnaesite accounts for approximately 60% of the total rare earth minerals. When occurring as liberated particles, it exhibits massive and irregular morphologies, as shown in Figure 4 (a). A portion of bastnaesite forms intergrowths with minerals such as aegirine, fluorite, and apatite (Figure 4 (b)). A minor fraction exists as disseminated and encapsulated types, forming three-phase intergrowths with gangue minerals. Monazite has a finer dissemination size compared to bastnaesite and typically occurs as very fine particles, primarily in the form of phosphate. Its liberated particles are predominantly massive, as shown in Figure 4 (c). Some monazite grains are adjacently intergrown with minerals such as aegirine, fluorite, apatite, and hematite (Figure 4 (d)). A minor proportion of monazite forms multiphase intergrowths with quartz and bastnaesite.

Based on the above, over half of the rare earth minerals (predominantly bastnaesite and monazite) exist in liberated form, with the remainder intergrown with gangue minerals. Therefore, an open-circuit flotation process was prioritized. By optimizing the reagent regime and flowsheet configuration, the separation of both liberated and intergrown rare earth minerals was maximized, yielding an open-circuit flotation rare earth concentrate (primarily comprising liberated rare earth minerals) and middlings (dominated by intergrowths). Subsequently, the grinding fineness of the open-circuit flotation middlings was increased to achieve sufficient liberation of rare earth minerals from gangue. A closed-circuit flotation test was then conducted with an optimized flotation scheme, producing a closed-circuit flotation rare earth concentrate. Owing to the weakly paramagnetic property

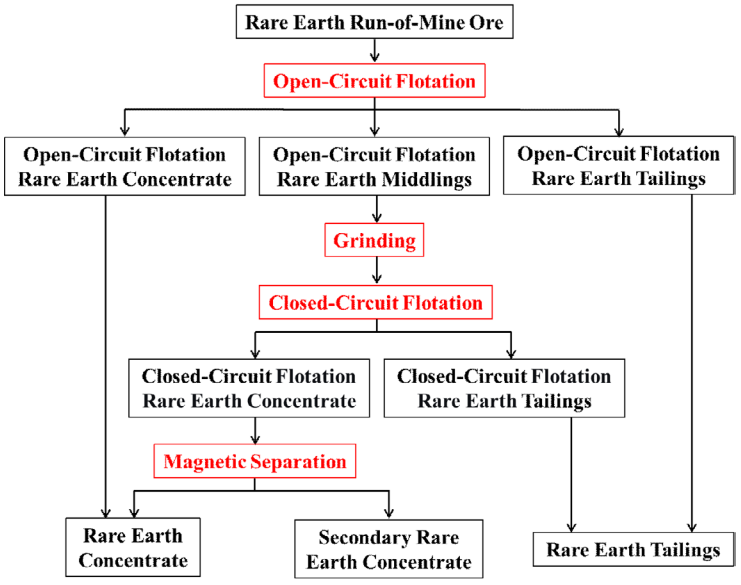

Fig. 5. Schematic flowsheet of the test

Rys. 5. Schematyczny przebieg badania

of rare earth minerals, magnetic separation was employed to further separate them from non-magnetic gangue minerals based on their magnetic susceptibility differences, resulting in a higher-grade rare earth concentrate. Consequently, a novel combined process of "open-circuit flotation – closed-circuit flotation of middlings – magnetic separation" was developed. Figure 5 illustrates the schematic flowsheet of this test.

3. Experimental study on the combined process of open-circuit flotation – closed circuit flotation of middlings – magnetic separation

ICP-OES/MS was employed to determine the REO grade in the products, calculate the REO recovery and yield, and thereby identify the optimal test conditions.

3.1. Optimization test results of open-circuit flotation process parameters for the rare earth ore

3.1.1. Flotation conditions optimization test

(1) Flotation environment optimization test

The flotation environment in this study, defined by pulp density, pulp pH, and temperature, serves as the critical external condition regulating mineral surface properties, reagent behavior, and bubble-particle interactions, thereby directly determining the selectivity and efficiency of the separation process.

Due to the high specific gravity of rare earth minerals, the flotation pulp density should be appropriately higher than that used for conventional minerals. An optimal pulp density is crucial for the effective beneficiation of rare earth ores. Tests were conducted at pulp densities of 40%, 45%, 50%, 55%, and 60%. Other constant conditions were: flotation temperature of 60°C, pulp pH of 9.16, depressant BY5 dosage of 1200 g/t, collector BQ2 dosage of 1200 g/t, and forther $2^{\#}$ oil dosage of 160 g/t. A single roughing flotation test was performed on the raw ore under each condition. The optimal condition was determined by comprehensively evaluating the REO grade, recovery, yield of the concentrate, and the REO grade of the tailings.

The test results are presented in Figure 6 (a). Both the REO grade and recovery in the concentrate initially increased and then decreased with rising pulp density. An appropriate increase in pulp density enhanced the interaction between rare earth minerals and flotation reagents, thereby improving REO grade and recovery. However, when the pulp density exceeded the optimal beneficiation concentration, the excessively high rare earth content per unit volume, combined with their high specific gravity, made it difficult for the pulp system to sustain continuous flotation. This caused a significant portion of the rare earth minerals

to settle, leading to a notable decline in both REO grade and recovery. Consequently, the optimal pulp density was determined to be 45%, achieving a concentrate REO grade of 22.81% and a recovery of 85.23%.

The beneficiation of rare earth minerals imposes stringent requirements on pulp pH, as both excessively high and low pH levels are detrimental to REO recovery. Thus, an optimal pulp pH is crucial for effective flotation. In this test, sodium carbonate served as the pH modifier while simultaneously exhibiting a certain activating effect on the rare earth minerals. The pulp pH was set to natural (6.96), 7.5, 8.0, 8.5, 9.0, and 9.5, respectively. The tests were conducted at a pulp density of 45%, with all other conditions remaining constant.

As shown in Figure 6 (b), the REO grade and recovery of the concentrate initially increased and then decreased with rising pH. When the pulp was alkaline, the collecting power of collector BQ2 towards the rare earth minerals was significantly weakened, leading to a substantial decline in both the REO grade and recovery of the concentrate. Consequently, the optimal pulp pH was determined to be 9.0, corresponding to a sodium carbonate dosage of 1000 g/t, which yielded a concentrate with an REO grade of 22.89% and a recovery of 85.28%.

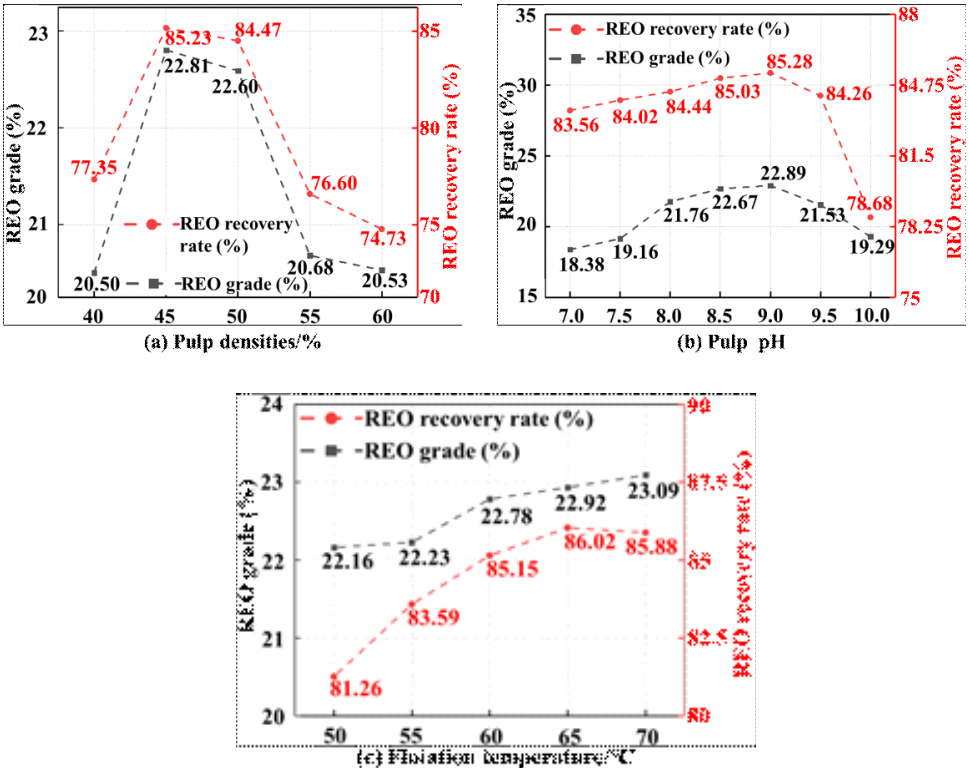

Fig. 6. Impact of the flotation environment on REO performance indicators

Rys. 6. Wpływ warunków flotacji na wskaźniki wydajności REO

Unlike conventional minerals that typically achieve satisfactory flotation performance at ambient temperature, rare earth minerals require heated flotation due to their distinctive physicochemical characteristics. To investigate the impact of temperature on rare earth flotation efficiency, tests were conducted at flotation temperatures of 50°C, 55°C, 60°C, 65°C, and 70°C. Under constant experimental conditions with pulp concentration maintained at 45% and pulp pH at 9, the effect of temperature on flotation performance is illustrated in Figure 6 (c). As the flotation temperature increased, the REO grade of the concentrate showed a gradual improvement, while the recovery rate initially increased before declining. This phenomenon can be attributed to the enhanced selective adsorption of collectors on rare earth mineral surfaces at elevated temperatures, concurrently suppressing gangue minerals such as fluorite and barite. Consequently, the optimal flotation temperature was determined to be 65°C, under which the concentrate achieved an REO grade of 22.93% and a recovery rate of 86.02%.

(2) Reagent regime optimization test

Following the determination of the optimal flotation environment, the effects of depressant, collector, and frother types and their dosages on REO performance indicators were investigated. Tests were conducted using a single-stage roughing flotation process, with reagents added sequentially as follows: depressant (variable), collector BQ2 (1200 g/t), and $2^{\#}$ oil (160 g/t).

The tested depressant schemes included sodium silicate (Na_2SiO_3), BY5, a combination of sodium silicate and carboxymethyl cellulose (Na_2SiO_3 + CMC), and a mixture of sodium silicate and sodium fluorosilicate (Na_2SiO_3 + Na_2SiF_6). The specific depressant types and dosage schemes are detailed in Table 11, and the corresponding test results are presented in Figure 7.

Table 11. Depressant type scheme

Tabela 11. Schemat środka obniżającego

Number	Reagent name	Reagent dosage (g/t)
1	Na_2SiO_2	1,200
2	Na_2SiO_2	1,600
3	BY5	1,200
4	BY5	1,600
5	Na_2SiO_2 + CMC	1,000 + 200
6	Na_2SiO_2 + CMC	1,200 + 400
7	Na_2SiO_2 + Na_2SiF_6	1,000 + 200
8	Na_2SiO_2 + Na_2SiF_6	1,200 + 400

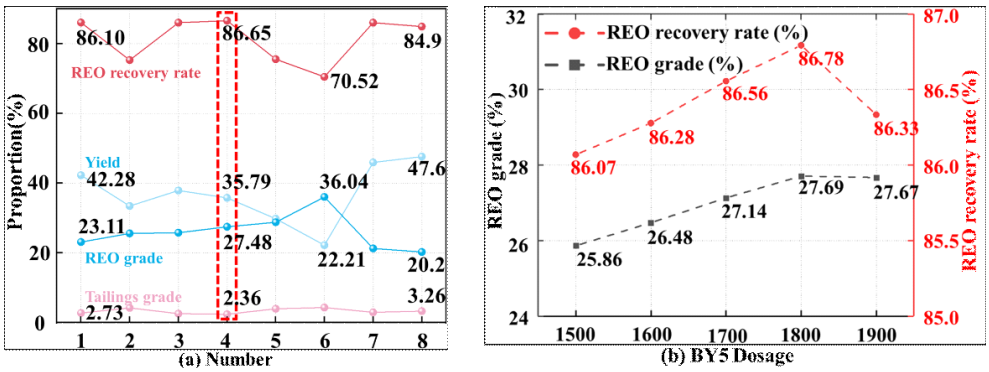

Fig. 7. Effect of depressant type and dosage on REO performance indicators

Rys. 7. Wpływ rodzaju środka obniżającego i dawki na wskaźniki wydajności REO

As shown in Figure 7 (a), the highest REO recovery in the concentrate, reaching 86.65%, was achieved with a BY5 depressant dosage of 1,600 g/t. Under this condition, the REO grade was 27.48%, the tailings REO grade was minimized at only 2.36%, and the yield was 35.79%. When using the combined depressant of sodium silicate and carboxymethyl cellulose, the concentrate REO grade reached a high value of 36.04%, but the recovery was only 70.52%. With the sodium silicate and sodium fluorosilicate combination, the concentrate yield was as high as 47.6%, but the REO grade was only 20.20%. Using sodium silicate alone as the depressant resulted in a concentrate REO grade of 23.11% and a recovery of 86.10%. Therefore, based on a comprehensive consideration of concentrate REO recovery, grade, and yield, BY5 was selected as the depressant for rare earth mineral separation. The optimization of the BY5 dosage is shown in Figure 7 (b). Both the REO grade and recovery in the concentrate exhibited a trend of first increasing and then decreasing with increasing BY5 dosage. The best performance indicators were achieved at a BY5 dosage of 1,800 g/t, yielding a concentrate REO grade of 27.69% and a recovery of 86.78%.

Following the determination of the BY5 depressant dosage, the type and dosage of the collector were varied. Under identical test conditions, BQ2, H203, and H205 were evaluated as collectors. The specific types and dosage schemes are detailed in Table 12, and the corresponding results are presented in Figure 8.

Table 12. Collector type scheme

Tabela 12. Schemat typu kolektora

Number	1	2	3	4	5	6
Reagent name	BQ2	BQ2	H203	H203	H205	H205
Reagent dosage (g/t)	1,000	1,200	1,000	1,200	1,000	1,200

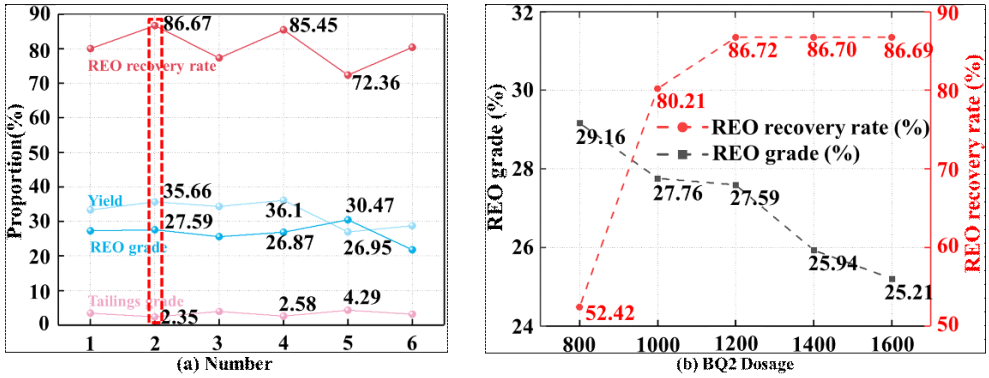

Fig. 8. Effect of collector type and dosage on REO performance indicators

Rys. 8. Wpływ rodzaju kolektora i dawki na wskaźniki wydajności REO

Figure 8(a) shows that at a BQ2 dosage of 1200 g/t, the concentrate achieved an REO recovery of 86.67%, a grade of 27.59%, a tailings grade of only 2.35%, and a yield of 35.66%. When using collector H203 at 1,200 g/t, the recovery was 85.45%, the grade was 26.87%, and the yield was 36.1%. With collector H205 at a dosage of 1,000 g/t, the REO grade reached 30.47%, but the recovery was only 72.36% with a yield of 26.95%. Based on a comprehensive evaluation, BQ2 was selected as the preferred collector for subsequent tests. With increasing BQ2 dosage, the REO grade of the concentrate gradually decreased, while the recovery initially increased rapidly and then stabilized. As shown in Figure 8(b), a BQ2 dosage of 1,200 g/t yielded favorable indicators, resulting in a concentrate REO grade of 27.59% and a recovery of 86.72%.

With the dosages of BY5 and BQ2 determined, the type and dosage of the frother were systematically varied. Under consistent experimental conditions, methyl isobutyl carbinol (MIBC), Q1-01ZY ($11^{\#}$ oil), and terpenic oil ($2^{\#}$ oil) were selected as frothers for evaluation. The specific frother types and corresponding dosage schemes are detailed in Table 13, and the test results are presented in Figure 9.

As illustrated in Figure 9(a), when $2^{\#}$ oil was used as the frother at a dosage of 200 g/t, both the REO recovery and yield of the concentrate reached their maximum values – achieving a recovery of 86.88% and a yield of 37.17% – while the tailings REO grade was 2.37%.

Table 13. Frother type scheme

Tabela 13. Schemat typów spieniaczy

Number	1	2	3	4	5	6
Reagent name	MIBC	MIBC	$11^{\#}$oil	$11^{\#}$oil	$2^{\#}$ oil	$2^{\#}$ oil
Reagent dosage (g/t)	160	200	160	200	160	200

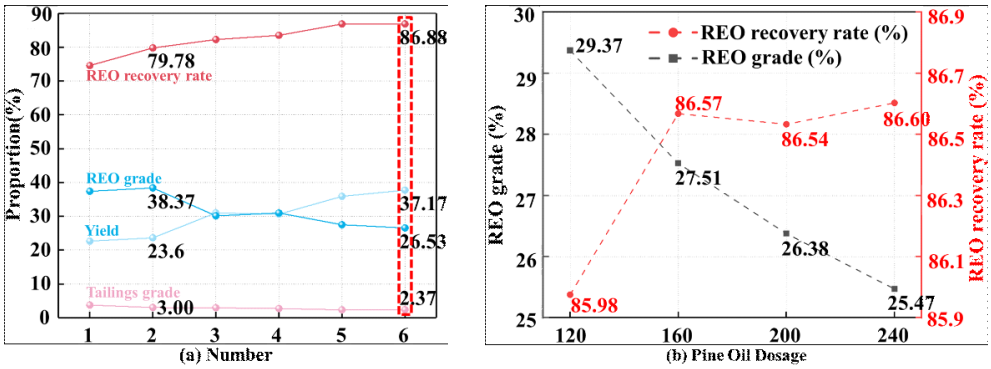

Fig. 9. Effect of frother type and dosage on REO performance indicators

Rys. 9. Wpływ rodzaju i dawki środka spieniającego na wskaźniki wydajności REO

In contrast, when MIBC was applied at the same dosage (200 g/t), the concentrate REO grade reached a higher value of 38.37%, but both the yield and recovery were comparatively lower. Therefore, 2# oil was selected as the more suitable frother for subsequent tests. Within the experimental range, the variations in concentrate REO grade and recovery were relatively modest. As shown in Figure 9(b), as the dosage of 2# oil increased, the REO grade exhibited a gradual decline, while the recovery initially increased and then stabilized. The optimal performance was achieved at a 2# oil dosage of 160 g/t, resulting in a concentrate REO grade of 27.51% and a recovery of 86.57%.

3.1.2. Flotation kinetics and flowsheet optimization tests

To determine the optimal flotation time for rare earth minerals, flotation kinetics tests were conducted on the raw ore. During the tests, products were collected at specific intervals: one product every 1 minute in the first roughing stage, one product every 2 minutes in the first scavenging stage, and one product every 2 minutes in the second scavenging stage. In the third scavenging stage, due to a significant reduction in froth volume observed experimentally, products were collected every 5 minutes. Figure 10 shows the test flowsheet, and the corresponding results are presented in Table 14.

Based on the experimental results presented in Table 14, the flotation rate was rapid within the first 5 minutes. As flotation time progressed, the increase in REO recovery exhibited a pattern of initially being fast and then slowing down. After 5 minutes of flotation, the incremental increase in REO recovery per minute fell below 2 percentage points, coupled with a significant reduction in froth volume. Consequently, the rougher flotation time was determined to be 5 minutes. During the first 2-minute interval of the first scavenging stage, the REO recovery increased by 2.76 percentage points. This was followed by an increase of

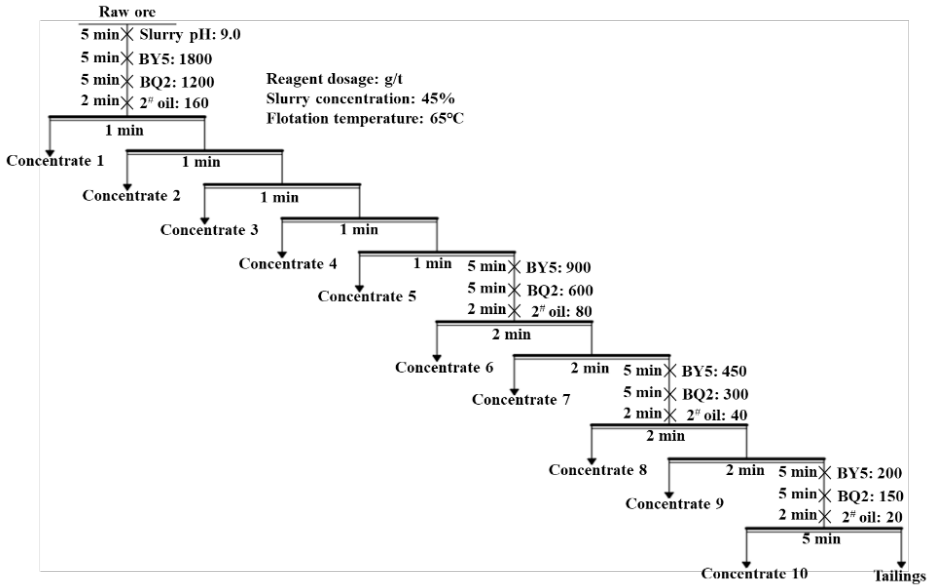

Fig. 10. Flotation kinetics test flowsheet

Rys. 10. Schemat procesu badania kinetyki flotacji

Table 14. Flotation kinetics test results

Tabela 14. Wyniki badań kinetyki flotacji

Flotation time/min	Product	Yield/%	REO grade/%	REO recovery rate/%
1	concentrates 1	15.54	31.69	43.39
2	concentrates 2	9.37	26.96	22.26
3	concentrates 3	6.19	24.22	13.21
4	concentrates 4	3.46	21.13	6.44
5	concentrates 5	1.38	11.93	1.45
7	concentrates 6	2.76	8.10	1.97
9	concentrates 7	1.39	5.23	0.64
11	concentrates 8	0.85	5.07	0.38
13	concentrates 9	0.52	4.37	0.20
18	concentrates 10	0.28	4.05	0.10
/	tailings	58.26	1.94	9.96
/	raw ore	100.00	11.35	100.00

only 1.39 percentage points in the second 2-minute interval. In the first 2-minute interval of the second scavenging stage, the recovery increased by a mere 0.85 percentage points, and by only 0.52 percentage points in the subsequent 2-minute interval. When the scraping interval was extended to 5 minutes in the third scavenging stage, the recovery increased by just 0.28 percentage points. Therefore, for this particular ore, further extending the number or duration of scavenging stages was deemed unnecessary. Based on the flotation kinetics test results, the optimal flotation parameters were determined as follows: a rougher flotation time of 5 minutes, followed by a single scavenging stage with a total duration of 4 minutes.

3.1.3. Cleaner circuit optimization and open-circuit flotation test

To investigate the optimal cleaner circuit configuration for rare earth mineral separation, multi-stage cleaning tests were conducted. The REO performance indicators of both the final concentrate and the cleaner tailings from each stage were measured. The test flowsheet

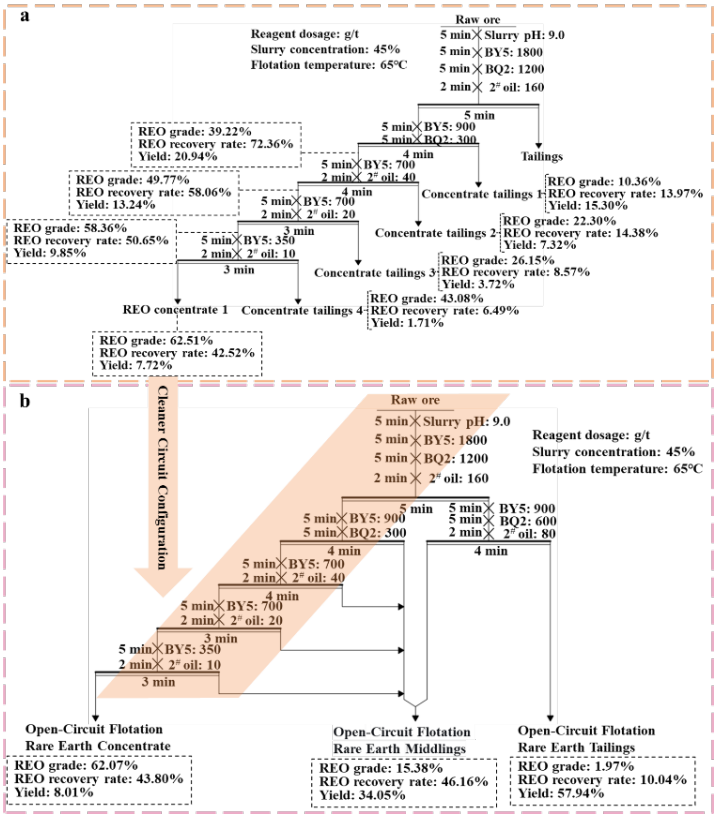

Fig. 11. Test of the cleaning circuit for the raw ore (a) and open-circuit flotation test (b)

Rys. 11. Badanie obwodu czyszczenia rudy surowej (a) oraz próba flotacji w obiegu otwartym (b)

and corresponding results are shown in Figure 11(a). The results indicate that the REO grade of the concentrate increased with the number of cleaning stages. Specifically, the REO grade achieved with two-stage cleaning was 10.55 percentage points higher than that with one-stage cleaning. This was further improved by 8.59 percentage points with three-stage cleaning, and by an additional 4.15 percentage points with four-stage cleaning. After four stages of cleaning, a concentrate REO grade of 62.51% could be achieved with a recovery of 42.52%. Considering the production capacity of existing rare earth processing equipment and the target requirements for both concentrate REO grade and recovery, it was determined that the cleaner circuit should consist of at least four stages.

Subsequent open-circuit flotation tests were conducted on the rare earth ore. The test flowsheet and corresponding results are presented in Figure 11(b). As shown in the results, under a grinding fineness of 90% passing 0.074 mm and using a "one roughing, one scavenging, and four cleaning" open-circuit flotation process, three final products were obtained:

1. Open-circuit flotation rare earth concentrate (grade: 62.07%, recovery: 43.80%, yield: 8.01%). This result aligns well with the liberation degree data of the two main rare earth minerals from process mineralogy studies, indicating that effectively liberated rare earth minerals were substantially recovered.
2. Open-circuit flotation rare earth middlings (grade: 15.38%, recovery: 46.16%, yield: 34.05%).
3. Open-circuit flotation rare earth tailings (grade: 1.97%, recovery: 10.04%, yield: 57.94%), corresponding to a low REO loss rate of only 10.04%.

3.2. Process optimization tests on closed-circuit flotation and magnetic separation of rare earth middlings

3.2.1. Condition testing for closed-circuit flotation of rare earth middlings

Based on the results of the open-circuit flotation tests on the rare earth ore, over 50% of the rare earth minerals were lost to the middlings and tailings. The dissemination characteristics of the rare earth minerals in the middlings are more complex than in the raw ore, with most rare earth minerals intergrown with gangue. Further improving the grinding fineness and increasing the degree of liberation of the rare earth minerals are necessary to enhance the beneficiation indicators. Therefore, a series of tests was conducted sequentially: grinding fineness optimization for the middlings, followed by dosage tests for depressant BY5, collector BQ2, and frother 2$^{\#}$ oil. The results of these tests are presented in Figure 12.

To investigate the effect of middlings fineness on the flotation performance of REO, the rare earth middlings were subjected to fine grinding using a vertical stirred mill.

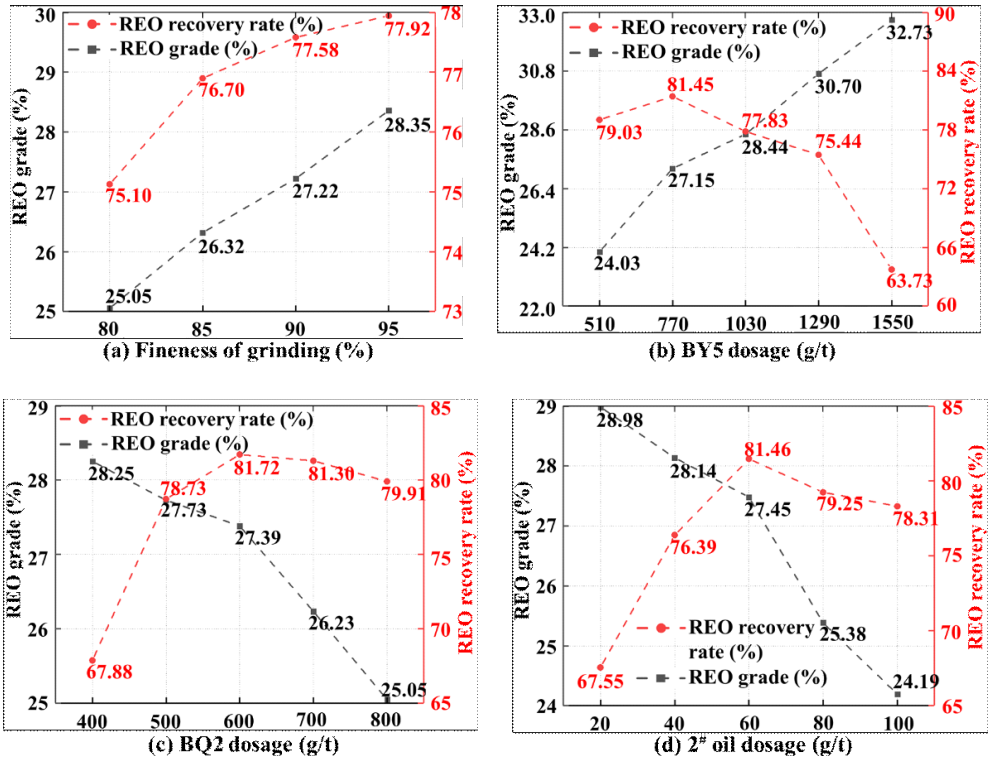

Fig. 12. Effect of different flotation conditions on REO performance indicators

Rys. 12. Wpływ różnych warunków flotacji na wskaźniki wydajności REO

The grinding fineness was set at four levels: 80%, 85%, 90%, and 95% passing 0.038 mm. Other test conditions remained constant: flotation concentration at 45%, pulp pH at 9.0, flotation temperature at 65°C, depressant BY5 dosage at 1050 g/t, collector BQ2 dosage at 600 g/t, and frother 2# oil dosage at 60 g/t. A single roughing flotation test was conducted under each condition. The impact of grinding fineness on rare earth concentrate indicators is shown in Figure 12(a). The results demonstrate that both the REO grade and recovery rate of the concentrate increased with finer grinding. This improvement can be attributed to the liberation of abundant moderately liberated and poorly liberated rare earth mineral particles in the middlings, which facilitates the effective recovery of rare earth minerals. Therefore, the optimal grinding fineness was determined to be 95% passing 0.038 mm, achieving an REO grade of 28.35% and a recovery rate of 77.92%.

With the grinding fineness fixed at 95% passing 0.038 mm, the depressant BY5 dosage was adjusted to 510 g/t, 770 g/t, 1,030 g/t, 1,290 g/t, and 1,550 g/t. The effect of depressant dosage on the concentrate indicators under identical test conditions is shown in Figure 12(b). The results indicate that the REO grade gradually increased with higher BY5 dosage. However,

excessive BY5 enhanced its interaction with rare earth minerals, thereby depressing their flotation and causing the operating recovery to rise slowly initially and then decline rapidly. Thus, a BY5 dosage of 770 g/t was identified as optimal, yielding a concentrate REO grade of 27.15% and an operating recovery of 81.45%.

With the grinding fineness fixed at 95% passing 0.038 mm and the BY5 dosage at 770 g/t, the collector BQ2 dosage was varied to 400 g/t, 500 g/t, 600 g/t, 700 g/t, and 800 g/t. The influence of collector dosage is shown in Figure 12(c). The REO grade decreased gradually with increasing BQ2 dosage, while the operating recovery initially increased and then stabilized. This is attributed to the simultaneous flotation of some gangue minerals along with the rare earth minerals at higher collector dosages, leading to a reduction in concentrate grade. Considering both REO grade and recovery, a BQ2 dosage of 600 g/t was selected as optimal, achieving a concentrate REO grade of 27.39% and an operating recovery of 81.72%.

With the grinding fineness fixed at 95% passing 0.038 mm, BY5 dosage at 770 g/t, and BQ2 dosage at 600 g/t, the $2^{\#}$ oil dosage was adjusted to 20 g/t, 40 g/t, 60 g/t, 80 g/t, and 100 g/t. The effect of $2^{\#}$ dosage is shown in Figure 12(d). The REO grade decreased with increasing $2^{\#}$ oil dosage, while the operating recovery first increased, then decreased, and finally stabilized. Higher $2^{\#}$ oil dosages generated excessive froth, which carried additional gangue minerals to the concentrate, thereby reducing the REO grade. Therefore, a $2^{\#}$ oil dosage of 60 g/t was determined to be optimal, resulting in a concentrate REO grade of 27.45% and an operating recovery of 81.46%.

3.2.2. Cleaning circuit and open-circuit test for rare earth middlings

To determine the optimal cleaning circuit configuration for rare earth middlings, multi-stage cleaning tests were conducted. The REO performance indicators of both the final concentrate and the cleaning tailings from each stage were measured. The test flowsheet and corresponding results are presented in Figure 13(a). The results demonstrate that the REO grade of the concentrate progressively increased with the number of cleaning stages. Specifically, the REO grade achieved with two-stage cleaning was 10.15 percentage points higher than that with one-stage cleaning. A further increase of 6.34 percentage points was achieved with three-stage cleaning, and an additional improvement of 4.32 percentage points was observed with four-stage cleaning. After four stages of cleaning, a concentrate REO grade of 59.49% and an operating recovery of 32.18% were obtained. Considering the production capacity of the available flotation equipment, it was determined that the cleaning circuit should comprise at least four stages.

Subsequently, open-circuit flotation tests were performed on the rare earth middlings. The test flowsheet and results are shown in Figure 15(b). The results indicate that under a grinding fineness of 95% passing 0.038 mm and using a “one roughing and four cleaning” open-circuit flotation process, a rare earth concentrate with an operating yield of 8.25%, an REO grade of 59.69%, and an operating recovery of 32.02% was obtained, along with

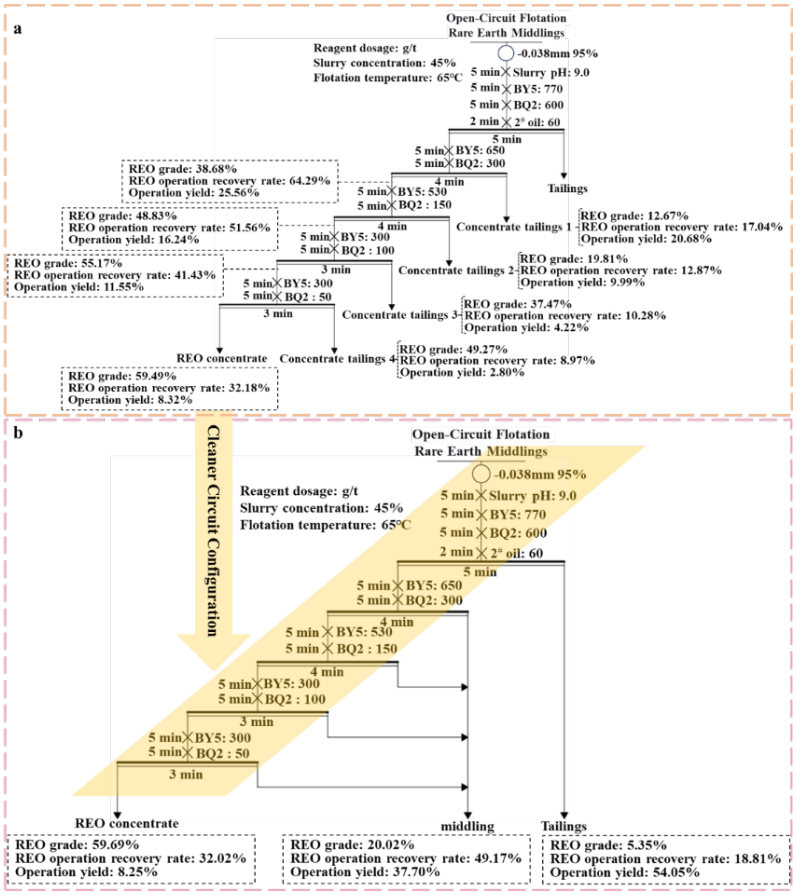

Fig. 13. Optimization of the medium ore selection (a) and open-circuit test (b)

Rys. 13. Optymalizacja doboru rudy średniej jakości (a) oraz próba w obiegu otwartym (b)

an intermediate product exhibiting an operating yield of 37.70%, an REO grade of 20.02%, and an operating recovery of 49.17%.

3.2.3. Closed-circuit flotation and magnetic separation optimization tests for rare earth middlings

Based on the open-circuit flotation tests conducted on the rare earth middlings, closed-circuit flotation tests were subsequently carried out. The test flowsheet and corresponding results are presented in Figure 14.

As shown by the results in Figure 14, under a grinding fineness of 95% passing 0.038 mm, the “one roughing-four cleaning” closed-circuit flotation process applied to the

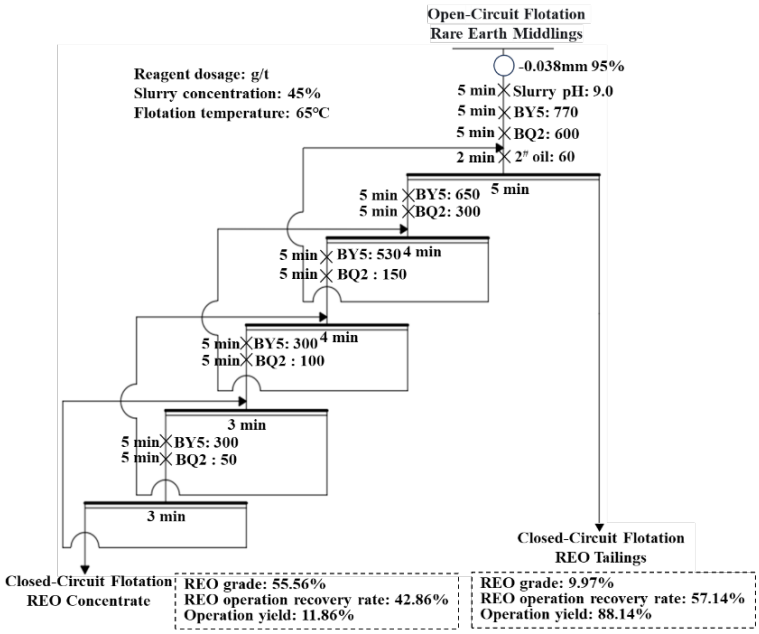

Fig. 14. Flowsheet and results of the closed-circuit flotation test on rare earth middlings

Rys. 14. Schemat technologiczny i wyniki próby flotacji w obiegu zamkniętym frakcji pośredniej metali ziem rzadkich

rare earth middlings sample yielded a rare earth concentrate with an operating yield of 11.86%, an REO grade of 55.56%, and an operating recovery of 42.86%, alongside tailings with an operating yield of 88.14%, an REO grade of 9.97%, and an operating recovery of 57.14%. Compared with the open-circuit flotation process, the closed-circuit flotation increased the operating yield of the rare earth concentrate by 3.61 percentage points, decreased the grade by 4.13 percentage points, and significantly enhanced the operating recovery by 10.84 percentage points, thereby achieving more efficient recovery of the rare earth concentrate.

3.2.4. Magnetic separation test on the closed-circuit flotation REO concentrate

Based on the results of the closed-circuit flotation tests on the rare earth middlings, the grade of the obtained rare earth concentrate remains relatively low. BPMA analysis revealed that this concentrate still contains a significant proportion of impurity minerals, including iron-bearing minerals, fluorite, apatite, barite, etc. Some of these impurities are magnetic, while others are non-magnetic, whereas the rare earth minerals themselves are weakly paramagnetic. The differing magnetic properties of these minerals allow for their

further separation using magnetic separation equipment, thereby upgrading the rare earth concentrate grade and producing a higher-quality product.

If strongly magnetic minerals in the concentrate prematurely enter a high-gradient magnetic separator, they can easily cause pore clogging in the matrix, adversely affecting the separation efficiency. Therefore, it is necessary to first remove these strongly magnetic minerals via low-intensity magnetic separation, followed by high-gradient magnetic separation to further reduce the content of non-magnetic impurities. This study investigates the beneficiation effectiveness of high-gradient magnetic separation applied to the closed-circuit flotation concentrate from the rare earth middlings. The magnetic separation flowsheet and corresponding results for the closed-circuit flotation concentrate are presented in Figure 15.

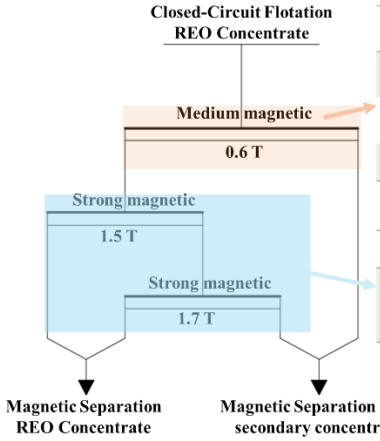

Name	Operational yield /%	REO grade /%	REO Operating recovery /%	Tfe grade/%	Tfe recovery/%
Magnetic concentrate	4.91	50.35	4.45	7.89	14.46
Magnetic separation tailings	95.09	55.83	95.55	2.41	85.54
Closed-circuit flotation concentrate	100.00	55.56	100.00	2.68	100.00

Magnetic field strength	Name	Operational yield /%	REO grade /%	REO Operating recovery /%
1.5T+1.7T	REO concentrate	82.43	58.07	85.74
	Tailings	17.57	45.31	14.26
	Closed-circuit flotation concentrate	100.00	55.83	100.00

Fig. 15. Flowsheet and results of the magnetic separation test on the closed-circuit flotation REO concentrate

Rys. 15. Schemat technologiczny i wyniki badania separacji magnetycznej koncentratu REO z flotacji w obiegu zamkniętym

(1) Low-intensity magnetic separation test

The results in Figure 15 show that after low-intensity magnetic separation, the iron grade in the magnetic concentrate increased by 5.21 percentage points, while it decreased by 0.27 percentage points in the magnetic tailings. This indicates effective recovery of strongly magnetic iron minerals from the feed. Additionally, the rare earth grade in the magnetic tailings slightly increased by 0.27 percentage points, suggesting a preliminary enrichment of rare earth elements through this low-intensity magnetic separation step.

(2) High-intensity magnetic separation test

Following the medium-intensity magnetic separation, the tailings still contained weakly magnetic iron-bearing minerals such as aegirine and limonite. It is necessary to employ

high-intensity magnetic separation to remove these weakly magnetic iron-bearing minerals and further enhance the grade of the rare earth concentrate. The high-intensity magnetic separation tests were conducted using the tailings from the medium-intensity magnetic separation as the feed. The results in Figure 15 demonstrate that after one stage of high-intensity magnetic roughing (1.5 T) and one stage of high-intensity magnetic scavenging (1.7 T), a final rare earth concentrate with an REO grade of 58.07% and an operating recovery of 85.74% was obtained.

3.3. Full-circuit closed-circuit test of the rare earth ore

Based on all the flotation and magnetic separation conditions established in sections 4.1 and 4.2 of this chapter, a full-circuit test of the rare earth ore was conducted. The test flowsheet is shown in Figure 16, and the results are presented in Table 15.

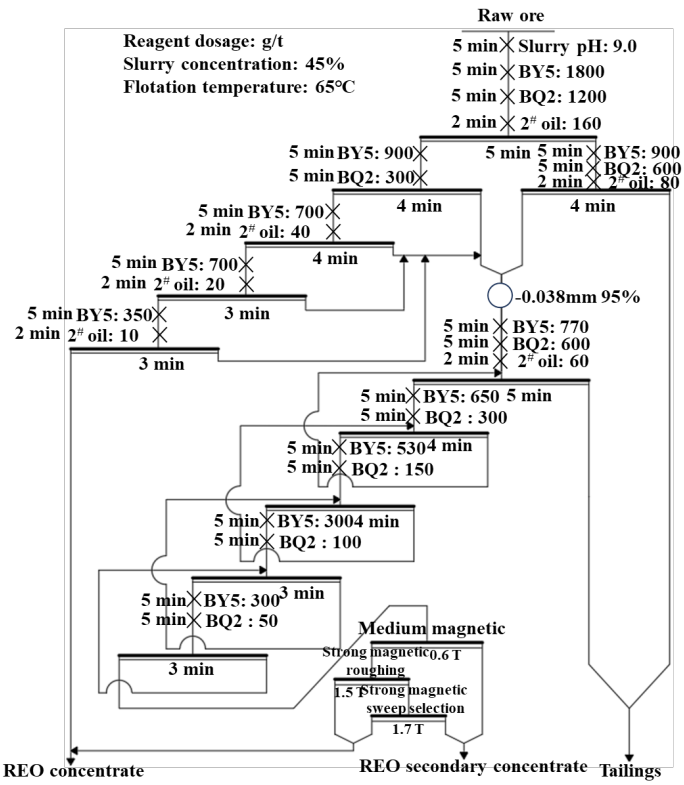

Fig. 16. Full-circuit closed-circuit test flowsheet

Rys. 16. Schemat przebiegu testu w obwodzie zamkniętym

Table 15. Full-circuit closed-circuit test results

Tabela 15. Wyniki testów w warunkach pełnego obwodu zamkniętego

Product name	Yield/%	REO grade/%	REO recovery/%
REO concentrate	10.62	61.09	57.15
REO secondary concentrate	1.43	50.98	6.42
Tailings	87.95	4.70	36.43
Raw ore	100.00	11.35	100.00

The data in Figure 16 and Table 15 demonstrate that through the combined process of "open-circuit flotation – closed-circuit flotation of middlings – magnetic separation", the rare earth ore yielded three products:

1) rare earth concentrate with a yield of 10.62%, an REO grade of 61.09%, and an REO recovery of 57.15%;
2) rare earth secondary concentrate with a yield of 1.43%, an REO grade of 50.98%, and an REO recovery of 6.42%;
3) rare earth tailings with a yield of 87.95%, an REO grade of 4.70%, and an REO recovery of 36.43%.

Compared with previous beneficiation processes, the REO grade of the rare earth concentrate increased by 6.09 percentage points, and its REO recovery improved by 12.45 percentage points. Meanwhile, the REO grade of the tailings decreased by 2.18 percentage points, with corresponding reductions in REO recovery and yield of 18.57 and 2.76 percentage points, respectively. These results confirm that the combined process significantly enhances the utilization efficiency of rare earth resources.

4. Mechanistic study on the depression of fluorite and barite by BY5

Flotation test results of the rare earth ore indicate that at pH = 9, BY5 can effectively act as a depressant for fluorite and barite during the flotation of bastnaesite, enabling efficient recovery of the rare earth minerals. To investigate the depression mechanism of BY5 on fluorite and barite, single mineral flotation tests were conducted using pure samples of bastnaesite, fluorite, and barite under three conditions: without depressant, with sodium silicate (water glass), and with BY5. Fourier transform infrared (FTIR) spectroscopy was analyzed under different test schemes to further elucidate the types of interfacial interactions involved. The test schemes are detailed in Table 16.

Table 16. Single mineral flotation test schemes

Tabela 16. Schematy badań flotacyjnych pojedynczych minerałów

Pure mineral	Reagent name	Dosage (mg/L)
Bastnaesite	BQ2	80
	Sodium silicate + BQ2	90 + 80
	BY5 + BQ2	120 + 80
Fluorite	BQ2	80
	Sodium silicate + BQ2	90 + 80
	BY5 + BQ2	120+80
Barite	BQ2	80
	Sodium silicate + BQ2	90 + 80
	BY5+BQ2	120 + 80

4.1. Single mineral flotation tests

4.1.1. Experimental scheme

To comprehensively illustrate the depressive effect of inhibitor BY5 on fluorite and barite in the bastnaesite-BQ2 system, control tests were conducted without a depressant and with sodium silicate as a depressant. The specific test schemes are as follows:

1. Effect of collector BQ2 concentration: the influence of BQ2 concentration (0, 20 mg/L, 40 mg/L, 60 mg/L, 80 mg/L) on the flotation behavior of the three pure minerals was investigated. After adding BQ2, the pulp was stirred for 2 min, followed by the addition of 20 mg/L methyl isobutyl carbinol (MIBC) as a frother. The pulp was stirred for an additional 1 min before froth scraping. The flotation time was 3 min, and both froth products and tank residues were collected to determine the optimal BQ2 concentration.
2. Effect of sodium silicate concentration: after determining the optimal BQ2 concentration, the influence of sodium silicate concentration (0, 30 mg/L, 60 mg/L, 90 mg/L, 120 mg/L) on the flotation behavior of the three pure minerals was studied. Sodium silicate was added and stirred for 2 min, followed by BQ2 addition and stirring for 2 min. Finally, 20 mg/L MIBC was added, and the pulp was stirred for 1 min before froth scraping. The flotation time was 3 min.
3. Effect of BY5 concentration: after determining the optimal BQ2 concentration, the influence of BY5 concentration (90, 100, 110, 120, 130 mg/L) on the flotation behavior

of the three pure minerals was examined. BY5 was added and stirred for 2 min, followed by BQ2 addition and stirring for 2 min. Finally, 20 mg/L MIBC was added, and the pulp was stirred for 1 min before froth scraping. The flotation time was 3 min.

4.1.2. Analysis of experimental results

All tests were repeated three times, and the average values were taken as the final flotation results. The flotation performance of the three minerals under different depressant conditions is shown in Figure 17.

Figure 17 (a) demonstrates that in the absence of a depressant, the recoveries of all three pure minerals gradually increased as the BQ2 concentration was raised from 0 to 80 mg/L.

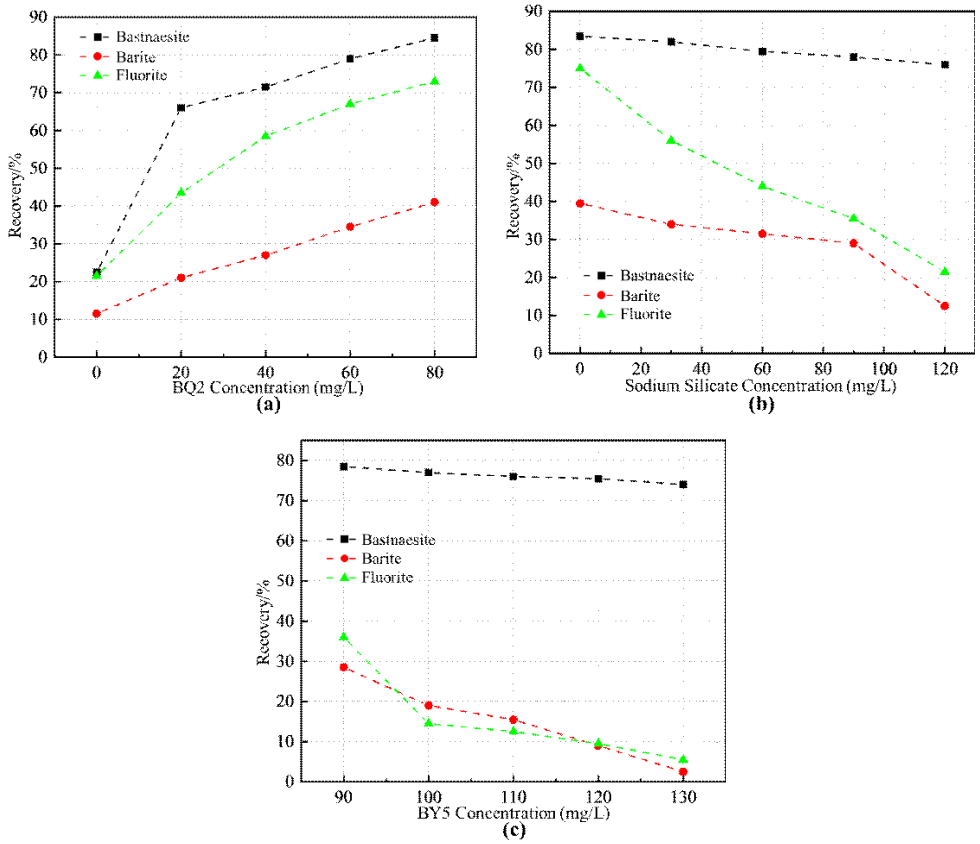

Fig. 17. Flotation recovery of three minerals under different depressants:
(a) no depressant, (b) with sodium silicate, (c) with BY5

Rys. 17. Odzysk trzech minerałów metodą flotacji przy zastosowaniu różnych środków obniżających:
(a) bez środka obniżającego, (b) z krzemianem sodu, (c) z BY5

Throughout this range, bastnaesite consistently exhibited higher recovery than both fluorite and barite. The recovery of barite increased at a relatively slow rate, reaching a maximum of approximately 41%. These results indicate that BQ2 possesses weaker collecting power toward barite and exhibits a certain degree of selectivity, enabling preliminary flotation separation of bastnaesite from barite. However, the similar floatability of fluorite and bastnaesite made their separation difficult. Consequently, a BQ2 concentration of 80 mg/L was selected for subsequent tests, where depressants were introduced to achieve separation among all three minerals.

As shown in Figure 18 (b), sodium silicate exerted a strong depressive effect on fluorite and barite. When the sodium silicate concentration was increased from 0 to 120 mg/L, the recovery of fluorite decreased by 37 percentage points, while that of barite decreased by 9.5 percentage points. In contrast, the recovery of bastnaesite declined by only 5 percentage points. This suggests that sodium silicate alone can effectively depress fluorite but shows limited inhibitory effect on barite.

From Figure 18 (c), it is evident that BY5 strongly depressed both fluorite and barite, with a more pronounced effect on the latter. As the BY5 concentration increased from 90 mg/L to 130 mg/L, the flotation recovery of bastnaesite decreased marginally from 85% to 80% across the tested range. In comparison, the recoveries of fluorite and barite dropped sharply by 57 and 30 percentage points, respectively, with both final recoveries falling below 10%. This confirms that the BY5 depressant effectively suppresses both fluorite and barite, thereby achieving efficient separation of all three minerals.

4.2. Analysis of FTIR results

4.2.1. FTIR analysis of bastnaesite before and after reagent interaction

The FTIR spectra of bastnaesite before and after reagent interactions are presented in Figure 18, where curve (a) represents pure bastnaesite, curve (b) corresponds to bastnaesite after full interaction with collector BQ2, curve (c) shows bastnaesite after treatment with depressant sodium silicate and collector BQ2, and curve (d) displays bastnaesite after interaction with depressant BY5 and collector BQ2.

As shown in Figure 18, the characteristic absorption peaks of bastnaesite are located at 1,422 cm^{-1}, 1,427 cm^{-1}, 1,090 cm^{-1}, 880 cm^{-1}, 859 cm^{-1}, and 718 cm^{-1}. The peaks at 1,422 cm^{-1} and 1,427 cm^{-1} are attributed to the asymmetric stretching vibration of carbonate ions, the peak at 1,090 cm^{-1} belongs to the symmetric stretching vibration of carbonate ions, while the peaks at 880 cm^{-1} and 859 cm^{-1} are assigned to the out-of-plane bending vibration, and the peak at 718 cm^{-1} corresponds to the in-plane bending vibration of carbonate ions. After interaction with collector BQ2 alone, two new absorption peaks emerged in the bastnaesite spectrum at 2,922 cm^{-1} and 2,852 cm^{-1}, which are characteristic

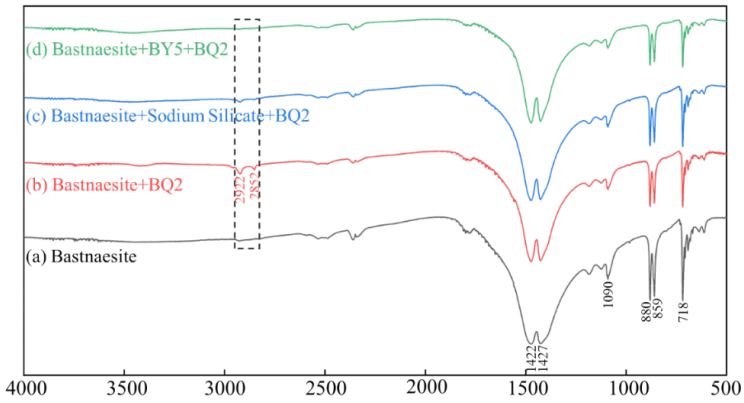

Fig. 18. FTIR spectra of bastnaesite before and after reagent interaction

Rys. 18. Widma FTIR bastnazytu przed i po oddziaływaniu z odczynnikiem

of the stretching vibrations of -CH_2- groups. This indicates that BQ2 underwent chemical adsorption or reaction with the bastnaesite surface, forming a hydrophobic layer. When sodium silicate was added as a depressant, no new absorption peaks were observed compared to the spectrum of pure bastnaesite. This suggests that sodium silicate adsorbs physically on the bastnaesite surface in the presence of BQ2. However, the intensity of the peaks at 2,922 cm^{-1} and 2,852 cm^{-1} decreased compared to the spectrum with BQ2 alone, indicating that sodium silicate partially hinders the adsorption of BQ2 on bastnaesite. In the case of BY5 addition, the absorption peaks at 2,922 cm^{-1} and 2,852 cm^{-1} nearly disappeared, demonstrating that BY5 more significantly prevents the adsorption of BQ2 onto bastnaesite. This result, combined with the absence of new peaks, confirms that BY5 interacts with bastnaesite primarily through physical adsorption.

4.2.2. FTIR analysis of fluorite before and after reagent interaction

The FTIR spectra of fluorite before and after reagent interactions are presented in Figure 19. Curve (a) represents pure fluorite, curve (b) corresponds to fluorite after full interaction with collector BQ2, curve (c) shows fluorite after treatment with depressant sodium silicate and collector BQ2, and curve (d) displays fluorite after interaction with depressant BY5 and collector BQ2.

As shown in Figure 19, the characteristic absorption peaks of fluorite are located at 3,440 cm^{-1}, 1,631 cm^{-1}, 1,439 cm^{-1}, and 878 cm^{-1}. The peaks at 3,440 cm^{-1} and 1,631 cm^{-1} are attributed to the O-H stretching vibration and H-O-H bending vibration, respectively, indicating the presence of adsorbed water in the sample. The peaks at 1,439 cm^{-1} and 878 cm^{-1} are assigned to the asymmetric stretching vibration and out-of-plane bending

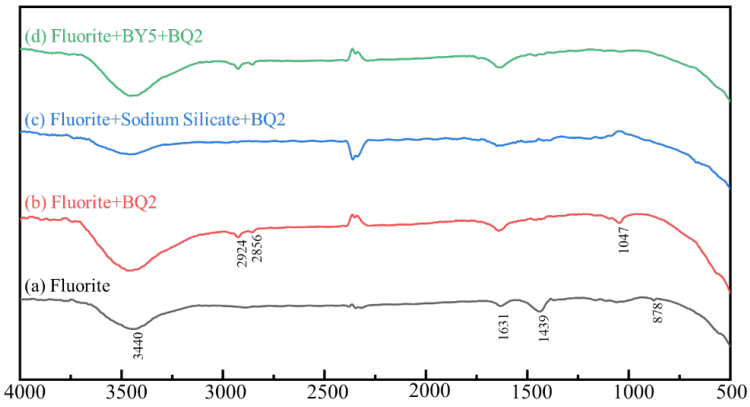

Fig. 19. FTIR spectra of fluorite before and after reagent interaction

Rys. 19. Widma FTIR fluorytu przed i po oddziaływaniu z odczynnikiem

vibration of carbonate ions, confirming the presence of calcite impurity in the sample. After interaction with collector BQ2 alone, new absorption peaks emerged in the fluorite spectrum at 2,924 cm^{-1}, 2,856 cm^{-1}, and 1,047 cm^{-1}. The peaks at 2,924 cm^{-1} and 2,856 cm^{-1} are characteristic of the stretching vibrations of -CH_2- groups, while the appearance of the peak at 1,047 cm^{-1} suggests the formation of Ca-O coordinate bonds through chemical adsorption between BQ2 and fluorite. When sodium silicate was added as a depressant, the peaks at 2,924 cm^{-1}, 2,856 cm^{-1}, and 1,047 cm^{-1} became nearly invisible. This demonstrates that sodium silicate prevents the adsorption of BQ2 on the fluorite surface through competitive adsorption and surface coverage, thereby effectively depressing fluorite. In the case of BY5 addition, compared to the spectrum of fluorite with BQ2 alone, distinct peaks appeared at 2,924 cm^{-1} and 2,856 cm^{-1}, while the absorption peak at 1,047 cm^{-1} disappeared. This indicates that BY5 chemically adsorbs onto fluorite and hinders the specific chemical adsorption of BQ2, though some physical adsorption of BQ2 may still occur.

4.2.3. FTIR analysis of barite before and after reagent interaction

The FTIR spectra of barite before and after reagent interactions are presented in Figure 20. Curve (a) represents pure barite, curve (b) corresponds to barite after full interaction with collector BQ2, curve (c) shows barite after treatment with depressant sodium silicate and collector BQ2, and curve (d) displays barite after interaction with depressant BY5 and collector BQ2.

As shown in Figure 20, the characteristic absorption peaks of barite are located at 1,180 cm^{-1}, 1,120 cm^{-1}, 1,083 cm^{-1}, 981 cm^{-1}, 635 cm^{-1}, and 610 cm^{-1}. The peaks at 1,180 cm^{-1} and 1,120 cm^{-1} are attributed to the asymmetric stretching vibration of sulfate ions,

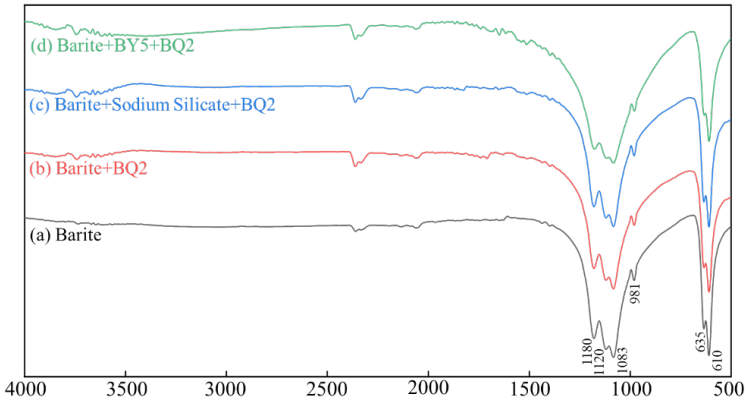

Fig. 20. FTIR spectra of barite before and after reagent interaction

Rys. 20. Widma FTIR barytu przed i po reakcji z odczynnikiem

representing the strongest characteristic peaks of barite. The peak at 1,083 cm^{-1} is assigned to the symmetric stretching vibration of sulfate ions, confirming the crystalline structure. The peak at 981 cm^{-1} is associated with other vibrational modes of sulfate ions, possibly arising from lattice vibrations, and its presence further enriches the spectral features of barite. The peaks at 635 cm^{-1} and 610 cm^{-1} are attributed to the asymmetric bending vibration of sulfate ions. After interaction with collector BQ2 alone, no new absorption peaks appeared in the infrared spectrum. The probable explanation is that the adsorption of collector BQ2 on the barite surface is dominated by weak physical interactions (e.g., electrostatic adsorption, hydrogen bonding, or van der Waals forces). While such adsorption can influence the mineral's flotation behavior, the alteration of barite's surface chemical properties is too subtle to produce discernible characteristic peaks in the infrared spectrum. When sodium silicate was added as a depressant, it forms negatively charged silicic acid colloids or ions in aqueous solution, which adsorb onto the barite surface through electrostatic interactions or hydrogen bonding. This leads to competitive adsorption with collector BQ2. Such physical adsorption does not generate new characteristic peaks in the infrared spectrum, as the Si-O stretching vibration may severely overlap with the peaks of sulfate ions in barite and thus remain indistinguishable. In the case of BY5 addition, silicate and citrate ions undergo rapid weak coordination with barium sites on the barite surface, preferentially occupying adsorption sites available for BQ2. This chemical adsorption occurs due to the stronger affinity of BY5 components, and since the collector exhibits weaker competitiveness, it cannot fully displace these depressant species. Consequently, the adsorption of BQ2 on barite is partially hindered.

4.3 Analysis of adsorption results

Under the condition of pulp pH 9 and collector BQ2 concentration of 80 mg/L, the effects of depressant BY5 concentration (0, 40, 80, 120, 160 mg/L) on the adsorption of collector BQ2 on pure mineral surfaces, and the effects of BY5 concentration (40, 80, 120, 160, 200 mg/L) on the adsorption of BY5 itself on pure mineral surfaces were investigated. The adsorption capacity was calculated according to Equation 1:

$$\tau=(C_0-C)\cdot\frac{V}{M} \tag{1}$$

- τ – adsorption capacity, mg/g,
- C_0 – initial reagent concentration, mg/L,
- C – residual reagent concentration, mg/L,
- V – solution volume, L,
- M – mineral mass, g.

The effect of BY5 concentration on BQ2 adsorption on mineral surfaces is shown in Figure 21(a), and the effect of BY5 concentration on its own adsorption on mineral surfaces is shown in Figure 21(b).

As seen in Figure 21(a), as BY5 concentration increases, the adsorption of BQ2 on bastnaesite, fluorite, and barite surfaces decreases to varying degrees. When BY5 concentration increases from 0 mg/L to 160 mg/L, BQ2 adsorption on fluorite decreases from 0.87 mg/g to 0.11 mg/g (a reduction of 0.76 mg/g), on barite from 0.72 mg/g to 0.17 mg/g (a reduction of 0.55 mg/g), and on bastnaesite from 0.91 mg/g to 0.64 mg/g

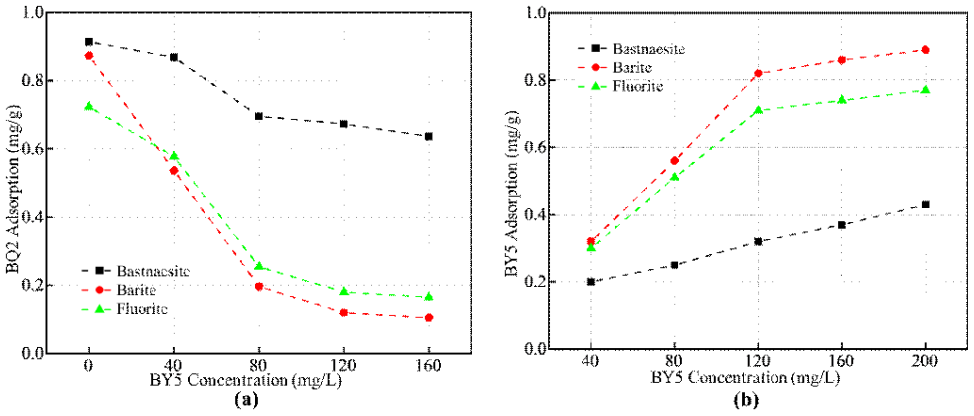

Fig. 21. Effect of BY5 concentration on the adsorption capacity of BQ2 (a) and BY5 (b) on mineral surfaces

Rys. 21. Wpływ stężenia BY5 na zdolność adsorpcyjną BQ2 (a) i BY5 (b) na powierzchniach mineralnych

(a reduction of only 0.27 mg/g). This indicates that increasing BY5 concentration has a significant impact on BQ2 adsorption on fluorite and barite surfaces, but a relatively small effect on BQ2 adsorption on bastnaesite. At a BY5 concentration of 120 mg/L, the adsorption of BQ2 on bastnaesite, fluorite, and barite surfaces is 0.67 mg/g, 0.12 mg/g, and 0.18 mg/g, respectively, with a maximum adsorption difference of 0.55 mg/g. Combined with FTIR analysis results, this demonstrates that BY5 and BQ2 undergo competitive adsorption on fluorite and barite surfaces, leading to reduced collecting ability of BQ2 toward fluorite and barite, which is consistent with the pure mineral flotation test results.

As shown in Figure 21(b), as the depressant BY5 concentration increases from 40 mg/L to 200 mg/L, the adsorption of BY5 on the three mineral surfaces gradually increases and eventually stabilizes. The adsorption of BY5 on fluorite increases from 0.32 mg/g to 0.89 mg/g (an increase of 0.57 mg/g), and on barite from 0.30 mg/g to 0.77 mg/g (an increase of 0.47 mg/g). In contrast, the adsorption of BY5 on bastnaesite increases slowly with increasing depressant concentration, rising only from 0.20 mg/g to 0.43 mg/g (a change of 0.23 mg/g). At a BY5 concentration of 120 mg/L, the adsorption of BY5 on bastnaesite, fluorite, and barite surfaces is 0.32 mg/g, 0.82 mg/g, and 0.71 mg/g, respectively. These results are consistent with the experimental findings on the effect of BY5 concentration variation on mineral depression.

Conclusions

This study investigates the Bayan Obo rare earth ore and achieves effective recovery of rare earth elements through a combined process of "open-circuit flotation – closed-circuit flotation of middlings – magnetic separation".

1. The rare earth ore contains 11.35% REO, predominantly composed of the four light rare earth elements La, Ce, Pr, and Nd. Their corresponding oxides (La_2O_3, CeO_2, Pr_6O_{11}, Nd_2O_3) account for a combined distribution of 97.80%. The primary rare earth minerals are bastnaesite and monazite, constituting over 85% of the total rare earth minerals. The dissemination grain size of bastnaesite and monazite is extremely fine; more than half exist as liberated particles, while the remainder is either encapsulated in gangue or present as intergrowths with other minerals. Consequently, these non-liberated particles report to the tailings and cannot be efficiently recovered, leading to low recovery and grade of the rare earth concentrate.
2. Using the open-circuit flotation flowsheet of "one roughing, one scavenging, and four cleaning" stages under the conditions of pulp density 45%, pH 9.0, flotation temperature 65°C, depressant BY5 dosage 1,800 g/t, collector BQ2 dosage 1,200 g/t, and frother (terpineol) dosage 160 g/t, a rare earth concentrate with an REO grade of 62.07% and REO recovery of 43.80% was obtained from the raw rare earth ore.
3. Applying the closed-circuit flotation flowsheet of "one roughing and four cleaning" stages to the rare earth middlings under the conditions of grinding fineness 95%

passing 0.038 mm, pulp density 45%, pH 9.0, flotation temperature 65°C, depressant BY5 dosage 770 g/t, and collector BQ2 dosage 600 g/t, a rare earth concentrate with an REO grade of 55.56% and an operational recovery of 42.86% was obtained. Subsequent open-circuit magnetic separation of this concentrate via "one roughing and one scavenging" stages yielded a final rare earth concentrate with an REO grade of 58.07% and an operational recovery of 85.74%.

4. The overall closed-circuit tests conducted on the rare earth ore using the combined process of "open-circuit flotation – closed-circuit flotation of middlings – magnetic separation" yielded a primary rare earth concentrate with a yield of 10.62%, REO grade of 61.09%, and REO recovery of 57.15%, along with a secondary rare earth concentrate with a yield of 1.43%, REO grade of 50.98%, and REO recovery of 6.42%. Compared to previous beneficiation processes, the REO grade of the primary concentrate increased by 6.09 percentage points, and its REO recovery increased by 12.45 percentage points. Concurrently, the REO grade in the tailings decreased by 2.18 percentage points, the REO recovery to tailings decreased by 18.57 percentage points, and the yield of tailings decreased by 2.76 percentage points. This combined process effectively enhances the utilization rate of rare earth resources and provides a scientific basis for improving the onsite rare earth beneficiation process.
5. The study on the depression mechanism of inhibitor BY5 reveals that BY5 chemisorbs on fluorite and barite surfaces but undergoes non-chemical adsorption on bastnaesite surfaces. Collector BQ2 chemisorbs on the bastnaesite surface. BY5 competes with BQ2 for adsorption sites on fluorite and barite surfaces, thereby hindering the adsorption of BQ2 on these gangue minerals.

We acknowledge the financial support provided by the National Key Research and Development Program of China (NO.2022YFC2905302); National Natural Science Foundation of China (52174236).

The Authors have no conflict of interest to declare.

REFERENCES

Chen et al. 2013 – Chen, Y., Song, Y., Wen, J., et al. 2013. Beneficiation of a Complex Niobium Ore Containing Rare Earths and Zirconium. *Chinese Journal of Rare Metals* 37(3), pp. 429–436.

Deng et al. 2024. – Deng, M.,Gao, H., Liu, J. et al. 2024. Biological Functions of Rare Earth Elements and Their Applications in Animal Production. *Chinese Journal of Animal Nutrition* 36(2), pp. 789–797.

Dutta et al. 2016 – Dutta, T., Kim, K.H., Uchimiya, M., Kwon, E.E., Jeon, B.H., Deep, A. and Yun, S.T. 2016. Global demand for rare earth resources and strategies for green mining. *Environmental Research* 150, pp. 182–190, https://doi.org/10.1016/j.envres.2016.05.052.

Fan et al. 2020 – Fan, H., Niu, H., Wang, Q., Yang, Z., Li, X. and Yang, K. 2020. The types, ore genesis and resource perspective of endogenic REE deposits in China. *Chinese Science Bulletin* 65(33), pp. 3778–3793, https://doi.org/10.1360/TB-2020-0432.

Goldschmidt, J.C. and Fischer, S. 2015. Upconversion for Photovoltaics – a Review of Materials, Devices and Concepts for Performance Enhancement. *Advanced optical materials* 3(4), pp. 510–535, https://doi.org/10.1002/adom.201500024.

He et al. 2016 – He, X., Rao, J., Luo, C., et al. 2016. Flotation Mechanism of Modified Alkyl Hydroximic Acid on Bastnaesite. *Journal of the Chinese Society of Rare Earths* 34(2), pp. 244–251.

Hu et al. 2025 – Hu, A., Liang, F., Luo, X.,Wang, Y., Qiao, Z., He, X. and Shen, A. 2025. Development and applications of new techniques for tests of trace elements and rare earth elements in carbonate minerals. *Oil & Gas Geology* 46(2), pp. 365–376, https://doi.org/10.11743/ogg20250203.

Kanazawa, Y. and Kamitani, M. 2006. Rare earth minerals and resources in the world. *Journal of Alloys and Compounds* 408–412, pp. 1339–1343, https://doi.org/10.1016/j.jallcom.2005.04.033.

Li et al. 2002 – Li, F., Zeng, X. and Zhu, Y. 2002. Application of Collector L102in Changlan Rare Earth Dressing Plant. *Chinese Rare Earths* 6, pp. 1–5.

Liu et al. 2016 – Liu, M., Liu, Y., Li, X., et al. 2016. Beneficiation Test Research of a Complex Rare Metal Associated Ore. *Nonferrous Metals (Mineral Processing Section)* 6, pp. 60–64.

Qiu et al. 2015 – Qiu, X., Lu, Z., Cheng, Q., et al. 2015. Beneficiation Technology of a Rare Earth Ore in Sichuan. *Nonferrous Metals Engineering* 5(5), pp. 46–49.

U.S. Geological Survey. Statistics and information on the worldwide supply of, demand for, and flow of the mineral commodity group rare earths-scandium, yttrium, and the lanthanides. Rare Earths Statistics and Information | U.S. Geological Survey [Online:] https://www.usgs.gov/ [Accessed: 2026-06-01].

Wang et al. 2013 – Wang, J., Cao, Z., Li, J., et al. 2013. Optimization of Floatation Reagents for Rare Earth Ore in Dressing Plant of Bayan Obo Rare Earth Ore. *Metal Mine* 11, pp. 74–76.

Wang et al. 2017 – Wang, C., Hu, Z., Qiu, X., et al. 2017. Experimental Study on a Novel Combined Beneficiation Technique for Bastnaesite Type RE Ore Using Magnetic-Gravity-Flotation Separation. *Chinese Journal of Rare Metals* 41(10), pp. 1151–1158.

Wang et al. 2023 – Wang, L.,Wang, C., Li, L. and Yang, Y.M. 2023. Readsorption of rare earth elements during leaching process of ion-adsorption-type rare earth ore. *Rare Metals* 42(06), pp. 2113–2120, https://doi.org/10.1007/s12598-018-1162-3.

Wu et al. 2023 – Wu, W., Han, J. and Fang Y. 2023. Current situation analysis and development strategy of rare earth industry. *Powder Metallurgy Industry* 33(6), pp. 133–139.

Xingyi et al. 2003 – Xingyi, W., Ying, W. and Guanzhong, L. 2003. Effect of Lanthanum on Methanol Fuel Exhaust Deep Oxidation over Palladium Catalyst. *Journal of rare earths* 21(1), pp. 51–54.

Xiong, S. and Ma, C. 2003. Experimental Research on Flotation Separation of a Bastnasite-Type Rare-Earths Ore. *Multipurpose Utilization of Mineral Resources* 3, pp. 8–13.

Xiong et al. 2018 – Xiong, W., Deng, J., Chen, D., et al. 2018. Beneficiation Research on a Phosphorus-silicate-RE Ore. *Nonferrous Metals (Mineral Processing Section)* 3, pp. 57–61.

Xiong et al. 2018 – Xiong, W., Deng, J., Chen, B., Deng, S. and Wei, D. 2018. Flotation-magnetic separation for the beneficiation of rare earth ores. *Minerals Engineering* 119, https://doi.org/10.1016/j.mineng.2018.01.014.

Xu et al. 2015 – Xu, D., Wang, J., Li, B., et al. 2015. A New Procedure for Comprehensive Recovery of Minerals Containing Rare Earth and Iron from Bayan Obo Ores. *Journal of the Chinese Society of Rare Earths* 33(5), pp. 633–640.

Xu et al. 2020 – Xu, Y., Xu, L., Wu, H., Wang, Z., Shu, K., Fang, S. and Zhang, Z. 2020. Flotation and co–adsorption of mixed collectors octanohydroxamic acid/sodium oleate on bastnaesite. *Journal of Alloys and Compounds* 819, https://doi.org/10.1016/j.jallcom.2019.152948.

Yan, C. and Huang, X. 2024. Review on Research of Rare Earths Field in China in 2023. *Journal of the Chinese Society of Rare Earths* 42(3), pp. 381–418.

Zhang et al. 2017 – Zhang, Y., Lin, H., Dong, Y.B., Xu, X.F., Wang, X. and Gao, Y.J. 2017. Coupling relationship between multicomponent recovery of rare earth tailings. *Rare Metals* 36(3), pp. 220–228, https://doi.org/10.1007/s12598-015-0489-2.

Zhang et al. 2020 – Zhang, S., Zhang, L., Zhang, Y., et al. 2020. Summarize on rare earth mineral resources and their distribution at home and abroad. *Inorganic Chemicals Industry* 52(1), pp. 9–16.

Zhao et al. 2020 – Zhao, C., Chen, H. and Yue, X. 2000. Application of LF-8 and LF-6 Collectors in Rare Earth Beneficiation. *Chinese Rare Earths* 3.

A NEW PROCESS FOR HIGH-EFFICIENCY RARE EARTH ENRICHMENT IN BAIYUN EBO METAL ORES: A SYNERGISTIC OPTIMIZATION STUDY OF OPEN-CIRCUIT FLOTATION, CLOSED-CIRCUIT FLOTATION OF THE MIDDLE ORE AND MAGNETIC SEPARATION

Keywords

rare earth ore, process mineralogy, bastnaesite, adsorption mechanism

Abstract

To address the low utilization rate of rare earth resources in the Bayan Obo mining area of Baotou, Inner Mongolia, China, a systematic experimental study was conducted using a novel combined process of "open-circuit flotation – closed-circuit flotation of middlings – magnetic separation". The mechanism of depressant BY5 on mineral surfaces was investigated through Fourier Transform Infrared Spectroscopy (FTIR) analysis and Ultraviolet-Visible (UV) spectrophotometric adsorption capacity tests. The results demonstrate that under the conditions of grinding fineness 95% passing 74 μm, flotation temperature 65°C, pulp concentration 45%, and pulp pH 9, using BY5 as depressant, BQ2 as collector, and terpineol as frother, an open-circuit flotation concentrate with a grade of 62.07% and recovery of 43.80% was obtained through "one roughing, one scavenging, and four cleaning" stages. For the rare earth middlings, with grinding fineness 95% passing 38 μm and optimized reagent dosage, subsequent "one roughing and four cleaning" flotation tests followed by "one roughing and one scavenging" magnetic separation tests yielded an open-circuit magnetic separation concentrate with a grade of 58.07% and operational recovery of 85.74%. The combined concentrates showed an overall yield of 10.62%, a grade of 61.09%, and a recovery of 57.15%. Depressant BY5 exhibits non-chemical adsorption on bastnaesite surfaces, while collector BQ2 undergoes chemical adsorption. BY5 competes with BQ2 for adsorption sites on fluorite and barite surfaces, thereby hindering BQ2 adsorption on these gangue minerals and achieving effective separation of bastnaesite from fluorite and barite.

NOWY PROCES WYSOKOWYDAJNEGO WZBOGACANIA PIERWIASTKÓW ZIEM RZADKICH W RUDACH METALI Z BAIYUN EBO: BADANIE OPTYMALIZACJI SYNERGICZNEJ FLOTACJI W OBIEGU OTWARTYM, FLOTACJI W OBIEGU ZAMKNIĘTYM RUDY ŚREDNIEJ ORAZ SEPARACJI MAGNETYCZNEJ

Słowa kluczowe

rudy metali ziem rzadkich, mineralogia procesowa, bastnazyt, mechanizm adsorpcji

Streszczenie

W celu rozwiązania problemu niskiego stopnia wykorzystania zasobów pierwiastków ziem rzadkich w rejonie górniczym Bayan Obo w Baotou w Mongolii Wewnętrznej w Chinach przeprowadzono systematyczne badania eksperymentalne z wykorzystaniem nowatorskiego, połączonego procesu

obejmującego „flotację w obiegu otwartym – flotację frakcji pośredniej w obiegu zamkniętym – separację magnetyczną". Mechanizm działania środka obniżającego BY5 na powierzchniach minerałów zbadano za pomocą analizy spektroskopii w podczerwieni z transformacją Fouriera (FTIR) oraz spektrofotometrycznych testów zdolności adsorpcyjnej w zakresie ultrafioletu i światła widzialnego (UV). Wyniki pokazują, że w warunkach rozdrobnienia 95% frakcji poniżej 74 μm, temperatury flotacji 65°C, stężenia zawiesiny 45% i pH zawiesiny 9, przy zastosowaniu BY5 jako środka obniżającego, BQ2 jako środka zbierającego oraz terpineolu jako środka spieniającego, w wyniku „jednego etapu zgrubnego, jednego etapu oczyszczającego i czterech etapów czyszczących" uzyskano koncentrat flotacyjny w obiegu otwartym o zawartości 62,07% i odzysku 43,80%. W przypadku frakcji pośredniej metali ziem rzadkich, przy stopniu rozdrobnienia 95% przechodzącym przez sito 38 μm i zoptymalizowanym dawkowaniu odczynników, kolejne testy flotacyjne „jedno zgrubne i cztery oczyszczające", a następnie testy oddzielania magnetycznego „jedno zgrubne i jedno oczyszczające" dały koncentrat z oddzielania magnetycznego w obiegu otwartym o zawartości 58,07% i wydajności operacyjnej 85,74%. Łącznie koncentraty wykazały ogólną wydajność 10,62%, zawartość 61,09% i odzysk 57,15%. Środek obniżający BY5 wykazuje adsorpcję nie chemiczną na powierzchniach bastnazytu, podczas gdy środek zbierający BQ2 ulega adsorpcji chemicznej. BY5 konkuruje z BQ2 o miejsca adsorpcyjne na powierzchniach fluorytu i barytu, utrudniając w ten sposób adsorpcję BQ2 na tych minerałach skały płonnej i umożliwiając skuteczne oddzielenie bastnazytu od fluorytu i barytu.